catalysts

MDPI

Review

Application of Pillared Clays for Water Recovery

Rubi Romero

Centro Conjunto de Investigación en Química Sustentable UAEM-UNAM, Universidad Autónoma del Estado de México, km 14.5 Toluca-Atlacomulco Road, Toluca 50200, Mexico; rromeror@uaemex.mx

Abstract: In recent years, efforts have been made in developing new and more efficient water purification methods and the synthesis of catalysts with greater catalytic activity that are more stable and can be used in wide pH ranges. Pillared clays represent a viable alternative for removing organic contaminants. The clays, usually smectites, are modified by inserting inorganic pillars (Al, Zr, Cr, Fe, Ti, Ga, and Mn) between the layers of the clay, increasing its surface area, porosity, catalytic activity, and thermal stability. This review describes the importance of using pillared clays with different polyoxycations in Fenton, photo-Fenton, ozonation, wet catalytic oxidation of hydrogen peroxide, and photocatalysis processes. Pillared iron clays (Fe-PILCs) are promising catalysts capable of generating hydroxyl radicals that can oxidize organic contaminants, thus facilitating their removal. The current challenges of the PILC application at industrial scale are also discussed.

Keywords: wastewater; Fe-PILCs; Fenton; photo-Fenton; ozonation; catalytic wet oxidation of hydrogen peroxide; photocatalysis; hydroxyl radical

1. Introduction

Nowadays, addressing water pollution problems is of paramount importance to mitigate the environmental impact that different anthropogenic activities have had on bodies of water.

In 2010, the United Nations General Assembly recognized the human right to drinking water and sanitation as essential for human life, establishing in 2015 the new Sustainable Development Goal (SDG 6) "Ensure the availability and sustainable management of water and sanitation for all" [1]. Throughout these years, efforts have been made to involve politicians, nations, and interested groups in various water and sanitation projects to develop efficient technologies for water management.

Although many developed countries have achieved universal access to safe drinking water (73% of the global population in 2022), this situation is very different for many less developed regions [2]. Figure 1 shows the distribution of drinking water worldwide in 2022.

Drinking water from rivers, lakes, and ponds is noticeably different from wastewater in terms of contamination extent [3]. Wastewater recovery and purification are critical challenges in environmental management and human health preservation, particularly as global water demand continues to increase due to urbanization, industrialization, and agriculture, among other activities generating large quantities of untreated or insufficiently treated wastewater [4,5], often containing highly water-soluble carcinogens, heavy metals [4], and other contaminants. This is worrying due to its high negative impact on ecosystems [6], since in high concentrations, it can cause severe diseases in humans and in both aquatic and terrestrial animals.

Academic Editor: Enric Brillas

Received: 28 December 2024
Revised: 28 January 2025
Accepted: 7 February 2025
Published: 9 February 2025

Citation: Romero, R. Application of Pillared Clays for Water Recovery. *Catalysts* **2025**, *15*, 159. https://doi.org/10.3390/catal15020159

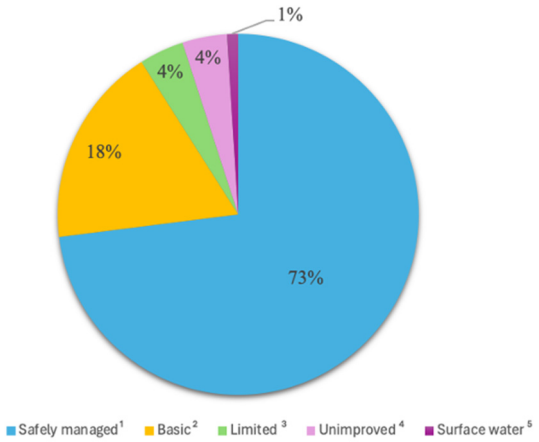

Figure 1. Distribution of access to drinking water worldwide with data from [2]. [1] Optimize water source available on site, accessible whenever required, and free from contaminants. [2] Optimize water source with a round-trip collection time of 30 min or less. [3] Optimize water source with a round-trip collection time exceeding 30 min. [4] Spring or well dug without any protection. [5] Drinking water coming directly from rivers, reservoirs, lakes, ponds, streams, canals, or irrigation systems.

For the above, efficient treatment processes are necessary to eliminate the various pollutants in water, which result from discharges of different anthropogenic activities (industries, agriculture, hospitals, and households) [7,8].

The treatment of wastewater is crucial for sustainable development and requires effective treatment systems. Currently, there are a handful of methods and technologies for wastewater treatment, which are usually divided into primary, secondary, and tertiary treatment techniques (Figure 2), which frequently incorporate biological, physical, and chemical procedures.

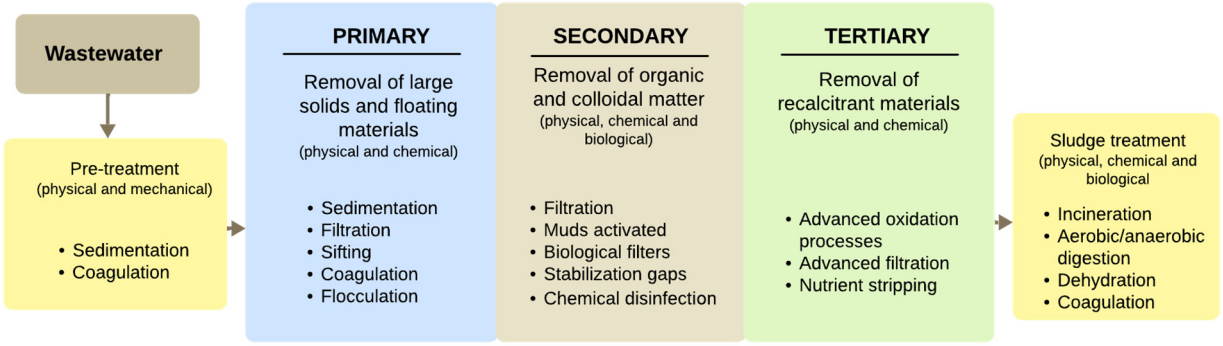

Figure 2. Levels of wastewater treatment.

The election of treatment typically relies on factors such as wastewater characteristics, cost, feasibility, efficiency, environmental impact, and operational challenges [3].

Advanced oxidation processes (AOPs), used as tertiary treatments, represent a viable option for water recovery since they are based on the generation of radicals with high oxidation–reduction potential such as hydroxyl radical (2.8 V), for the oxidative decomposition of contaminants, using low chemical consumption, and in most of the cases, eliminating sludge formation [3,9,10].

Due to their stability, catalytic activity and relatively easy recovery, heterogeneous catalysts are generally preferred in advanced oxidation processes. They are easily separated from the reaction mixture, can be used in successive runs, do not generate sludge, and are effective in a wide pH range.

Different supports such as synthetic and natural zeolites, carbons, mesoporous silica materials (SBA-15, MCM-41), metal–organic frameworks (MOFs), and clays have been

used as main constituents of catalytic systems for advanced oxidation reactions (Fenton-heterogeneous, photo-Fenton, ozonation, catalytic wet oxidation of hydrogen peroxide (CWPO), and photocatalysis) for wastewater treatment. Figure 3 depicts the distribution of scientific articles in the literature regarding the use of heterogeneous catalysts in advanced oxidation processes to remove contaminants in water from 2020 to date, according to SCOPUS (search date: January 2025).

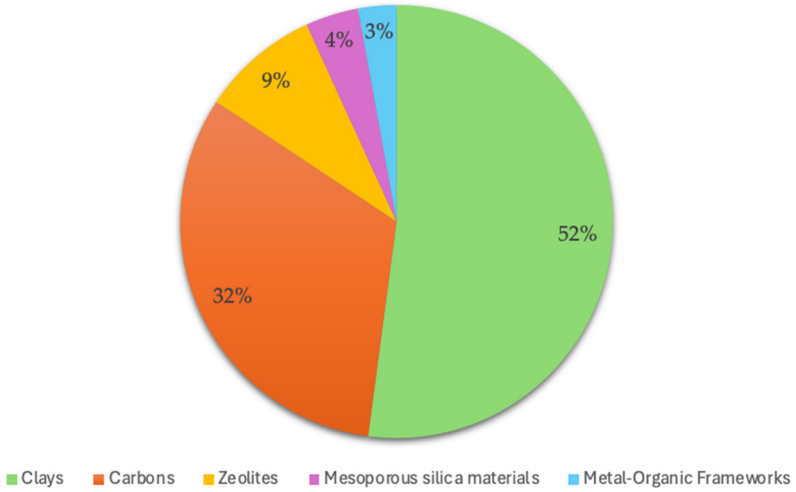

Figure 3. Supports employed in advanced oxidation processes for the removal of contaminants.

Figure 3 shows that the highest percentage of manuscripts dealing with catalyzed advanced oxidation processes focuses on clays as supports of catalytically active metals in the oxidation processes of organic compounds; for this reason, clays have become potential materials for the degradation of contaminants.

Clays are hydrated phyllosilicates ($Al_2Si_2O_5(OH)_4$) containing Fe^{3+}, Mg^{2+}, and other cations [11,12], forming a layered or sheet structure. These sheets are either tetrahedral or octahedral, the former being constituted by one Si atom bonded to four oxygen atoms (SiO_4), while octahedral sheets ($Al(Mg)O_8$) pose a high content of Al or Mg, bonded to oxygen atoms shared in different layers [12]. Due to the incomplete neutralization of oxygen, the clay layers have a negative charge, which is balanced by hydrated cations (Na^+, K^+, or Ca^+) located in the interlayer space [13].

Clay minerals are classified into a 1:1 type consisting of one tetrahedral and one octahedral sheet (kaolinite, halloysite, rectorite, chrysotile) and a 2:1 type consisting of two tetrahedral sheets and one octahedral sheet between them (smectites: laponite, bentonite, montmorillonite, sepiolite, laponite) [12,14]; the structure of the smectite is shown in Figure 4.

Clay minerals have been used in various processes to remove recalcitrant contaminants in solutions [16] and in a wide variety of industrial processes [13] due to their abundance, low cost, thermal stability, swelling properties, and environmental friendliness [17,18]. In addition, the interlayer space can be easily modified, increasing their porosity [19], which makes them excellent catalytic supports. The traditional process for increasing the porosity of clays is the pillaring method, where metallic polyoxocations are introduced in solution into the interlayer space. When dehydrated, the corresponding metallic oxide is obtained. Another alternative process is clay exfoliation, which consists of separating its layers using surfactants such as urea, hydrazine hydrate, formamide, potassium acetate, and *N*-methylformamide hydrate, causing a significant increase in the surface area, in mesopores and macropores [20–22]. In addition to presenting high thermal stability above 700 °C [23], this spacing that exfoliated clays presents allows them to be used mainly in adsorption

processes [17,24]. In the case of pillared clays, metallic species can be inserted into the interlayer space that provides catalytic activity to the material to be used in advanced oxidation processes.

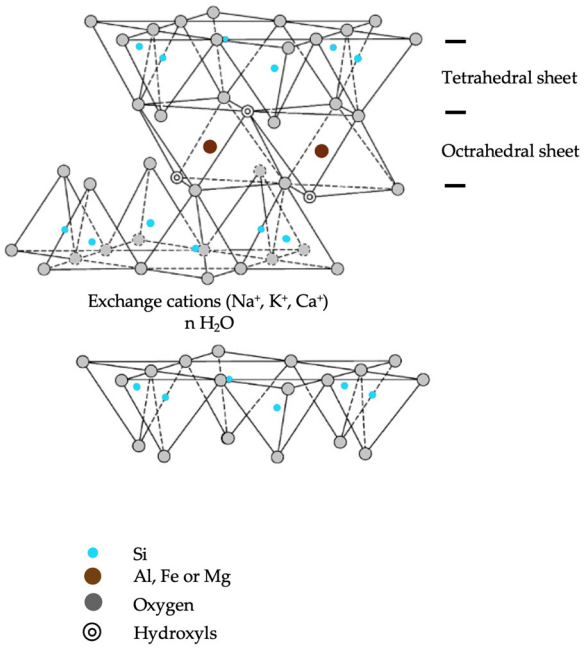

Figure 4. Structure of mineral clay 2:1 type (Smectite). Adapted with permission from [15]. Copyright 2025 Elsevier.

This review aims to summarize and analyze the use of pillared clays to remove organic contaminants in advanced oxidation processes, considering their effectiveness in Fenton, photo-Fenton, ozonation, catalytic wet hydrogen peroxide oxidation processes (CWPO), and photocatalytic reactions. It also describes the activity of pillared clays in water recovery and treatment in each of these processes.

2. Pillared Clays and Advanced Oxidation Processes

Advanced oxidation processes (AOPs) are a potential alternative for efficient wastewater treatment. These are based on the production and use of hydroxyl radicals (•OH) for decomposing organic or recalcitrant contaminants. These hydroxyl radicals are strongly reactive and not very selective [25], as well as being non-toxic. They are also potent oxidants (E^0 = 2.8 V) only below fluorine (E^0 = 3.03 V) and react between 10^6 and 10^{12} times faster than other oxidants such as ozone [26], achieving in most cases complete conversion of pollutants towards CO_2 and H_2O or partial mineralization and obtaining less-toxic intermediates [27]. Some of the most common AOPs include Fenton, photo-Fenton, ozonation, photocatalysis, electrochemical oxidation, and sonolysis [28,29].

2.1. Fenton Process

Fenton is an advanced oxidation process that employs iron salts (Fe^{2+}) to catalyze hydrogen peroxide (H_2O_2) dissociation in aqueous solution [27,30] to generate hydroxyl radicals (•OH) according to Equations (1) and (2),

$$Fe^{2+} + H_2O_2 \rightarrow Fe^{3+} + \bullet OH + OH^- \quad (1)$$

$$Fe^{3+} + H_2O_2 \rightarrow Fe^{2+} + H^+ + HO_2^{\bullet} \quad (2)$$

Equation (1) is considered the central reaction in the Fenton process where ferrous ions (Fe^{2+}) ($k_1 \approx 70\ M^{-1}\ s^{-1}$) [31] rapidly oxidize towards ferric ions (Fe^{3+}). Fe^{2+} ions are regenerated in Equation (2) with a slower rate constant (k_2 = 0.0001–0.01 $M^{-1}\ s^{-1}$) [32]. Also, the hydroperoxyl radical facilitates the regeneration of the ferrous ion, as shown in Equation (3) ($k_3 = 1.2 \times 10^6\ M^{-1}\ s^{-1}$) [33].

$$Fe^{3+} + HO_2^{\bullet} \rightarrow Fe^{2+} + O_2 + H^+ \quad (3)$$

In the Fenton process, the reaction time to mineralize organic compounds is shorter than other advanced oxidation methods [34]. Generally, this process occurs at pH 3, which promotes the generation of hydroxyl radicals (•OH) [35]; however, when pH increases, the iron oxyhydroxides and ferric hydroxide are produced, causing the precipitation of iron, i.e., sludge formation. Furthermore, the fact that the reaction rate of Equation (2) is slower than that of Equation (1) causes an excessive production of iron hydroxides, facilitating the formation of sludge [36].

When working at lower pH (<2), there is the presence of iron complex species $[Fe(H_2O)_6]^{2+}$ and stable oxonium ions $(H_3O_2)^+$, reducing the activity of Fe^{2+} and H_2O_2 [37]. The reaction rate in a Fenton process relies on the amount of iron, and the concentration of the oxidant directly influences the extent of contaminants mineralization, so the ratio of $[Fe^{2+}]_0/[H_2O_2]_0$ and the organic compounds affect the reaction pathways in the Fenton process [38]. Furthermore, other drawbacks of using homogeneous systems in Fenton processes are the high consumption of H_2O_2 [39], the addition of chemicals to maintain the acidic pH to ensure iron ions remain in solution [40], and the complicated recovery of iron from sludge, requiring additional treatments. This can be overcome by using heterogeneous iron catalysts, where the leaching of metal ions is low, they are more stable during the process, less dependent on pH, non-corrosive, easily recovered, environmentally friendly, and have higher activity [41]. In addition, these catalysts can easily be recovered from the reaction and reused in subsequent reactions [42].

Several studies suggest that Fenton reactions using heterogeneous catalysts occur on the surface of the catalysts or in layers very close to the surface. However, only some active sites are available to carry out Fenton reactions. Additionally, steric hindrance makes access to them difficult; one of the disadvantages of heterogeneous iron catalysts is the lower reaction rate compared to homogeneous catalysis [42,43].

The heterogeneous Fenton process involves three steps: (1) adsorption of organic compounds on the surface, (2) *in situ* generation and attack of •OH radicals on said compounds [44], and (3) desorption of the products from the catalyst surface [45]. Furthermore, the Fenton process can be enhanced with UV radiation or sunlight, a process known as photo-Fenton [46].

Application of Pillared Clays in Heterogeneous Fenton Processes

An innovative approach to improving water recovery processes is using pillared clays. These are modified clay materials with inorganic pillars inserted between the layers of natural clay. This alteration significantly increases the clay's structural stability, porosity and surface area, making it a highly effective medium for water treatment applications.

Pillared clays are porous materials obtained by exchanging cations of the clay (smectite) interlayers with inorganic polyoxocations (Al, Zr, Cr, Fe, Ti, Ga, and Mn) [25,47,48], which combine with oxygen to form stable metal oxide pillars [49]. Depending on the type of polyoxocation used, pillared clays can have different applications as adsorbents, photocatalysts, filler materials, etc. [16,50,51]. Inserting pillars between the clay layers alters the physiochemical characteristics and catalytic performance [52].

The basal spacing of clays is achieved when the polyoxocations are introduced. Through a calcination step, they are converted into pillars of metal oxides by dehydration and dihydroxylation, causing the interlayers to remain separated and preventing their collapse [53], as shown in Figure 5. Clays modified with pillars exhibit surfaces and microporosity of up to four times more than the clay without pillars [49], and have strong acidity and high thermal stability [54]. In general, it is known that Lewis acid sites in a pillared clay are located on the metal oxides that compose it. In contrast, Brönsted acid sites are in the structure of the clay layers associated with the OH groups, and the pillars also contribute to Brönsted acid sites [55,56]. In addition, due to the steric hindrance caused by the micropores formed, shape selectivity in these materials is facilitated [13].

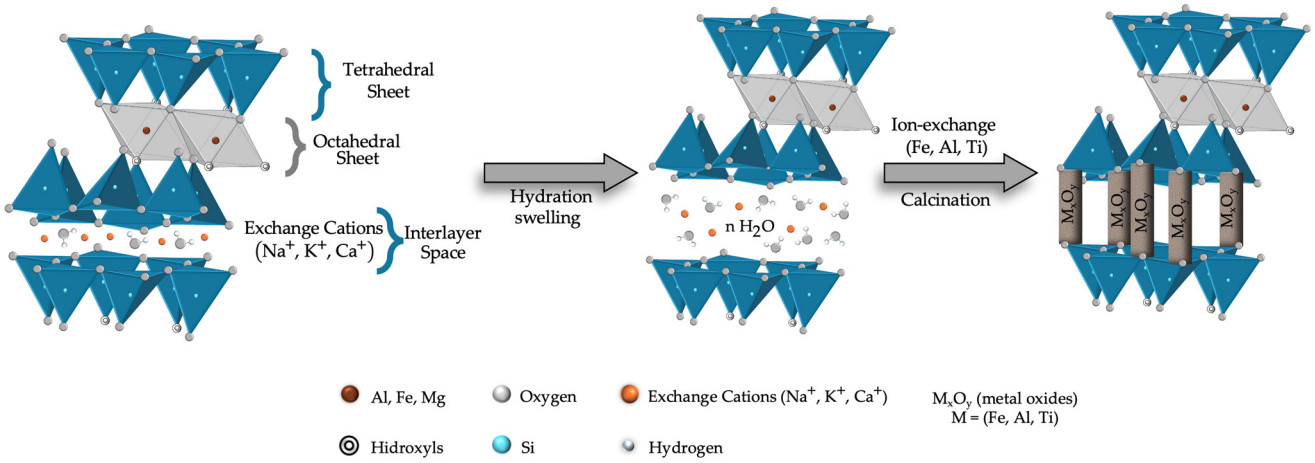

Figure 5. Schematic representation of the pillared clay process.

Pillared iron clays (Fe-PILCs) typically exhibit basal spacings of 21–25 Å (corresponding to $d_{0\,0\,1}$); this spacing includes the thickness of the laminae, which is 9.6 Å [57,58]. The formation of polymeric species of Fe_2O_3 permanently joins the sheets; these species are obtained when the Fe cations are dehydrated and dehydroxylated [57]. Previous works confirmed the presence of ferrous oxide (Fe^{2+}) and ferrous ferric oxide (Fe_3O_4) in Fe-PILCs. Fe_3O_4 (magnetite) is an oxide that contains a mixture of iron with two oxidation states (Fe^{2+}/Fe^{3+}) [58,59].

The catalytic action of the iron species of Fe-PILCs allows the generation of •OH radicals and thus achieves the elimination of organic compounds through the Fenton process. These iron-pillared clays in a Fenton process have efficiently degraded nitroaromatic compounds such as nitrobenzene [60]. Table 1 shows some of the studies using PILCs in Fenton processes for removal of organic compounds.

Table 1. Summary of iron-pillared clays for the Fenton process.

Organic Pollutants	Catalyst	Reaction Conditions	Remotion	Ref
Levofloxacin (LVX)	Iron-silica pillared clay	Catalyst loading = 0.5 g/L Concentration LVX = 50 mg/L pH = 3.0 Temperature = 40 °C 500 mg/L H_2O_2 Reaction time = 180 min in 5 consecutive runs	X_{LVX} = 90%	[61]

Table 1. *Cont.*

Organic Pollutants	Catalyst	Reaction Conditions	Remotion	Ref
Sulfanilamide (SA)	Fe, Al-Montmorillonite -pillared clay	Catalyst loading = 3 g/L Concentration SA= 0.29 mmol/L pH = 3.1 and 4.1 Temperature = 30–60 °C H_2O_2/SA = 1–36 mol/mol Reaction time = 360 min	X_{SA} = 95–99%	[62]
Cinnamic acid (CA)	Fe-bentonite	Concentration CA = 120 mmol/L pH = 2.9 Temperature = 80 °C Fe-cinnamic acid molar ratio = 10 H_2O_2/ molar ratio = 83 Reaction time = 60 min	X_{CA} = 90%	[63]
Pesticides (NPT)	Fe-pillared bentonite	Catalyst loading = 1 g/L Concentration NPT = 5 mg/L pH = 3.0 Temperature = 40 °C H_2O_2/NPT = 23.2 mg/L for 5 mg/L NPT	X_{NPT} = 100%	[64]
Nitrobenzene (NB)	Fe-pillared kaolinite	Catalyst loading = 1.0 g/L Concentration NB = 75 mmol/L pH = 3.0 ± 0.05 Temperature = 35 °C 10 mmol/L H_2O_2 Reaction time = 180 min 10 mmol/L H_2O_2	X_{NB} > 85%	[60]
Acid Green 25 (AG25)	Fe-Ipoh clay	Catalyst loading = 1.25 g/L Concentration AG25 = 50 mg/L pH = 3.0 Temperature = 30 °C 6.7 mM H_2O_2 Reaction time = 120 min	X = 95%	[65]
Orange II	Fe/pillared saponite	Catalyst loading = 90 mg/L Concentration Orange II = 0.1 mM pH = 3.0 Temperature = 70 °C 6 mM H_2O_2 Reaction time = 240 min	$X_{Orange\ II}$ = 91%	[66]
Orange II	Fe-Pillared bentonite clay (nanocatalysts)	Catalyst loading = 1 g Concentration Orange II = 0.2 mM pH = 3.0 Temperature = 30 °C 10 mM H_2O_2 Reaction time = 120 min	$X_{Orange\ II}$ = 100%	[67]

Table 1. *Cont.*

Organic Pollutants	Catalyst	Reaction Conditions	Remotion	Ref
Phenol	Al/Fe-pillared clay (bentonite)	Catalyst loading = 5 g/L Concentration Phenol = 5×10^{-4} mol/L pH = 3.7 Temperature = 25 °C 0.1 mol/L H_2O_2 Reaction time = 180 min	X_{phenol} = 100%	[68]
4-chlorophenol (4-CP)	Al/Fe-pillared clay (montmorillonite)	Catalyst loading = 0.5 g/L Concentration 4-CP = 155.6 µmol/L pH = 3.5 Temperature = 30 °C H_2O_2:4-CP = 13.5:1 (molar ratio) Reaction time = 240 min	$X_{4\text{-}CP}$ = 100%	[69]

As shown in Table 1, the use of iron-pillar clays employed in wastewater treatment allows for reaching high percentages of degradation of organic compounds in times of up to 6 h; in addition, using a pH of 3.0 allows the formation of hydroxyl radicals (•OH), but with the advantage of an easy recovery of the catalyst from the reaction medium [70]. It can also be observed that iron-pillared clays can remove a wide variety of organic compounds such as drugs, dyes, pesticides, and phenols. Furthermore, reaction temperatures are usually around 30 °C, since some authors [66] suggest that high reaction temperatures can decompose hydrogen peroxide into oxygen and water, affecting the mineralization time of organic compounds and favoring the leaching of iron, affecting the stability of the catalyst.

2.2. Photo-Fenton Processes

The photo-Fenton process is a variant of the typical Fenton process, where UV radiation (λ < 380 nm) or visible light (λ = 380–780 nm) is used to increase the efficiency of •OH generation, enhancing the process [71]. Additionally, UV radiation can help regenerate Fe^{2+} from Fe^{3+}, making the Fenton process more efficient. The regenerated Fe^{2+} reacts with H_2O_2 to form •OH radicals and Fe^{3+}.

The chemical reactions occurring in a photo-Fenton process are described by Equations (4)–(7) [72,73],

$$Fe^{3+} + hv \rightarrow Fe^{2+} + \bullet OH + H^+ \quad (4)$$

$$Fe^{2+} + H_2O_2 \rightarrow Fe^{3+} + \bullet OH + OH^- \quad (5)$$

$$H_2O_2 + hv \rightarrow 2(\bullet OH) \quad (6)$$

$$\bullet OH + \text{organic contaminants} \rightarrow \text{oxidized products} \quad (7)$$

2.2.1. Application of Pillared Clays in Heterogeneous Photo-Fenton Processes

Clays, as catalyst supports in the photo-Fenton process, offer a viable and reassuringly straightforward synthesis alternative due to iron's easy incorporation into their structure. Additionally, iron-pillared clays (Fe-PILCs) present an interesting option, thanks to their high stability and catalytic activity across a range of pH values from 3 to 7 [58,72,74]. This straightforward process and their high stability make them effective in treating various pollutants in wastewater, offering a promising future for wastewater treatment. As previ-

ously stated, Fe-PILCs have within their structure FeO (Fe^{2+}) and magnetite (Fe^{2+}/Fe^{3+}). Figure 6 schematically shows the photo-Fenton process employing iron-pillared clays.

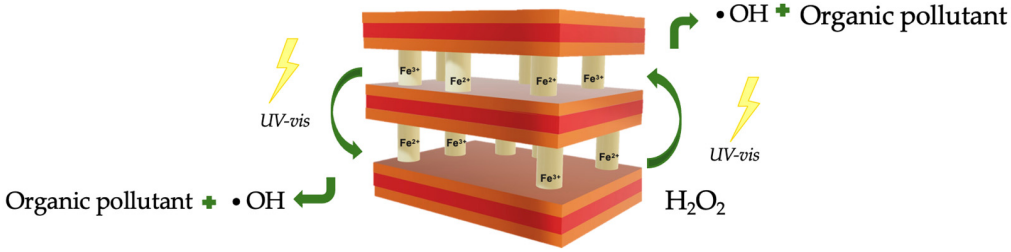

Figure 6. Schematic of the photo-Fenton process in Fe-PILCs.

Chen and Zhu [75] have proposed a simultaneous (heterogeneous–homogeneous) mechanism for the mineralization of Orange II using pillared iron clays (bentonite) under UV radiation. Firstly, for the heterogeneous mechanism, Fe^{3+} ions present on the clay surface are converted to Fe^{2+} by the effect of UV light (Equation (4)). Subsequently, the Fe^{2+} ions are oxidized by H_2O_2, forming OH radicals (Equation (5)). Likewise, the UV light favors the formation of more OH radicals (Equation (6)), which oxidize organic molecules (Orange II) (Equation (7)). They have also postulated that the formation of intermediate compounds (oxalic acid, phthalic acid, and 2-carboxybenzeneacetic acid) formed by the degradation of the dye in solution cause some iron ions to be leached, forming organic iron complexes that could be mineralized by oxidation of the hydroxyl radical and by a ligand-to-metal charge transfer (LMCT) process decarboxylating the organic intermediaries driven by photons. At the end of the cycle, these ions could return to the pillared clay's surface and continue the cycle, as seen in Scheme 1. These results also coincide with those proposed by Soon and Hameed [76] pillared iron clays based on laponite clay.

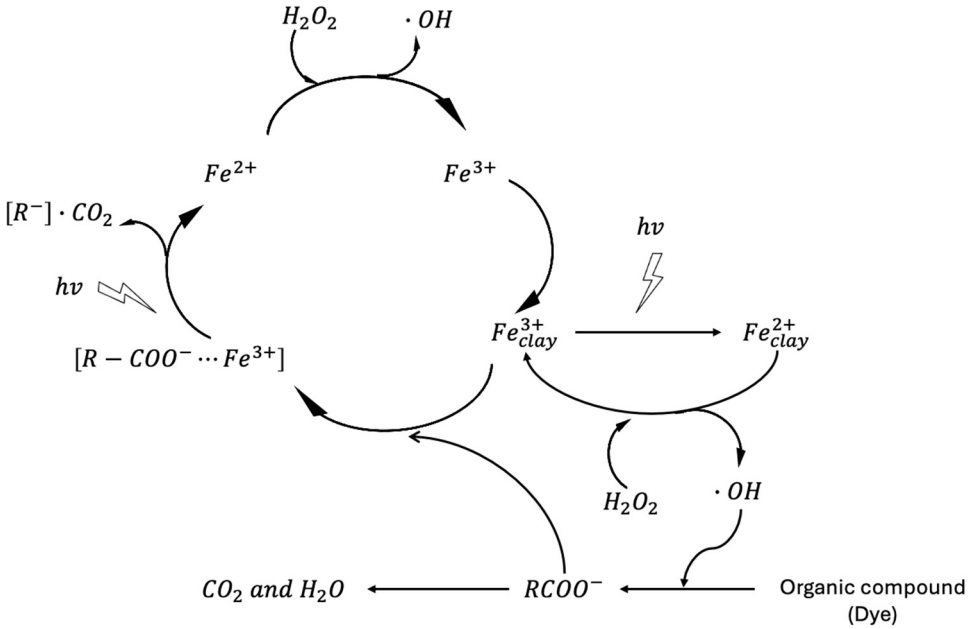

Scheme 1. Mechanism of photodegradation by UV radiation, including the Fe cycle. Adapted with permission from [75]. Copyright 2024 Elsevier.

According to Nidheesh et al. [77], the photo-Fenton process has advantages such as *(a)* reduction in the formation of iron sludge in comparison to the traditional Fenton process; *(b)* extra generation of hydroxyl radicals through the breakdown of H_2O_2; *(c)* swift production of ferrous ions (Fe^{2+}) when exposed to UV light.

Fe-PILCs have been used in photo-Fenton to remove organic compounds such as dyes (azo-dye Acid Black [78], azo-dye Orange II [79], Methylene Blue [80], Malachite Green and Red Congo [81], phenol [82], tyrosol [83], toluene [84], antibiotics [85], and other recalcitrant compounds. Some advantages of Fe-PILCs in photo-Fenton processes are their stability, their capacity to work with pH values higher than 3.0, and where leaching of Fe ions is minimal, which allows this type of catalyst to be used in various reaction cycles [25], extra generation of hydroxyl radicals through the breakdown of H_2O_2.

The Fe^{2+} and Fe^{3+} ions in the pillared iron clay structure allow oxidation reactions to occur at pH > 3.0, with negligible iron leaching [86,87]. Furthermore, iron as pillar is very active in forming •OH radicals.

Guo et al. [88] suggested using rectorite (clay material) and iron to simultaneously remove tetracycline hydrochloride and Cr(VI) in a pH range of 3.8–8.1 and sunlight. A degradation of 97.5% of tetracycline hydrochloride and 98.1% of Cr(VI) was obtained. The efficiency of these catalysts continued up to 5 reaction cycles, and their mesoporous structure facilitated the molecular diffusion of H_2O_2 and contaminants. Likewise, species such as goethite (Fe(OH)O) facilitated electron transfer, improving the removal of contaminants [89].

2.2.2. Influence of Copper in Fe-PILCs

As previously mentioned, Fe-PILCs have the advantage of working at pH > 3.0, and iron is very active in generating hydroxyl radicals. However, some authors [90] suggest that incomplete mineralization of organic products may occur when working at pH circumneutral, due to the formation of stable complexes. It is one of the reasons why some authors [58,91,92] propose the introduction of additional metals into iron-pillared clays, thus enhancing the efficiency of the photo-Fenton process and allowing the oxidation reactions to occur at pH values greater than 3.0.

Copper, aluminum, and titanium are some of the metals that have been incorporated into iron-pillared clays (Fe-PILCs) to carry out the removal of organic contaminants using photo-Fenton [58,93,94].

Copper as oxide is a Lewis acid that has very advantageous photocatalytic properties. It is a non-toxic material, is very stable over long periods, is environmentally friendly, and has strong light absorption [95].

Previous studies [76,96] have shown that, under acidic conditions, copper's catalytic activity is lower than iron's. However, copper shows higher catalytic activity under neutral or alkaline pH conditions. Furthermore, the interaction of Cu and Fe ions increases the generation of radicals [97], because the electron transfer in the reaction medium can be accelerated [95].

These effects have been reported by Khankhasaeva et al. [62] who employed pillared clays (Fe/Cu/Al-Montmorillonite) for total mineralization of sulfanilamide in 160 min and a pH value of 3.5–4.0, observing that the three-metal catalyst (Fe/Cu/Al-Montmorillonite) had higher activity than the two-metal systems (Cu/Al-Mt and Fe/Al-Mt); this is due to the interaction between copper and iron ions. Furthermore, the excellent stability of these catalysts allowed their reuse up to four times without losing notable catalytic activity (99–94%).

Hurtado et al. [58] reported the use of iron-pillared clays with copper (Cu/Fe-PILC) in the mineralization of paracetamol under neutral pH conditions by photo-Fenton process, obtaining about 80% mineralization at almost neutral pH conditions; this result was only 2% less than the degree of mineralization achieved at acidic pH after 180 min of reaction. Moreover, Hadjltaief et al. [94] reported the effectiveness of pillared iron clays doped with copper (Cu/Fe–PILC Tunisian clay) in mineralizing phenol. Their research, conducted

in the presence of UV–C irradiation and a range of pH from 3 to 7, showed that total mineralization was achieved after 40 min of reaction. The stability of the catalyst was maintained even after several reaction cycles (three times), and the leaching of the metals was insignificant (below 0.5 ppm), further confirming the effectiveness of the Cu/Fe-PILC catalyst.

Meijide et al. [89] mentioned that the stability of copper-/iron-pillared clays depends on the molar ratio of both metals (Fe-Cu), where copper is about 15 times less than iron.

As mentioned earlier, pillared clays have within their structure Brönsted and Lewis acid sites. This surface acidity favors the catalytic activity in the removal of organic pollutants. Dorado et al. [98] found that Fe-PILC has an acidity of 0.317 mmol NH_3/g, while a pillared iron clay with copper (Cu/Fe-PILC) (twice exchanged) shows a total acidity of 0.663 mmol NH_3/g. They proposed that the Na^+ ions present in Fe-PILC are replaced by Cu^{2+} (a Lewis acid cation). The ability of Cu²+ to be reduced to Cu^+ facilitates the reduction of Fe^{3+} to Fe^{2+}, thereby accelerating the production of •OH.

The above agrees with the work of Sun et al. [99], who proposed that in a Fe–Cu bimetallic catalyst, Fe^{2+} ions are primarily regenerated through the reaction between Fe^{3+} and Cu^+, as shown in Equation (8), instead of the reduction of Fe^{3+} and H_2O_2, as shown by Equation (2).

$$Cu^+ + Fe^{3+} \rightarrow Cu^{2+} + Fe^{2+} \quad (8)$$

Wei et al. [100] studied synthesizing magnetite (ferrous ferric oxide) for removing pyridine by the photo-Fenton process and circumneutral pH. Their findings suggest that the reaction of Cu^{2+} with H_2O_2 is a crucial factor in the production of more •OH radicals through their reduction to Cu^+ (Equation (9)). Likewise, this Cu^+ ion can also react with H_2O_2 and obtain Cu^{2+} and more hydroxyl radicals (•OH) (Equation (10)). Another way to obtain more hydroxyl radicals is when Cu^{2+} reacts with H_2O under UV radiation (Equation (11)).

$$Cu^{2+} + H_2O_2 \rightarrow Cu^+ + \ \bullet O_2^- + H^+ \quad (9)$$

$$Cu^+ + H_2O_2 \rightarrow Cu^{2+} + \ \bullet OH + OH^- \quad (10)$$

$$\equiv Cu^{2+} + H_2O + hv \rightarrow \equiv Cu^+ + \ \bullet OH + H^+ \quad (11)$$

Finally, another benefit of copper in iron catalysts is its role as a "protector" of iron, as reported by Zhang et al. [101]. They used copper in an acidic medium, where it reacted with oxygen to produce hydrogen peroxide. This hydrogen peroxide, a result of the copper's reaction, effectively prevents the iron from being oxidized, thereby ensuring the catalyst's effectiveness.

$$Cu^+ + O_2 + 2H^+ \rightarrow Cu^{2+} + H_2O_2 \quad (12)$$

2.3. Ozonation Processes

Ozonation is an advanced oxidation process, and a promising option for wastewater treatment. It efficiently eliminates refractory organic compounds in effluents from various industrial processes. Ozonation, unlike other AOPs, does not generate sludge, ensuring a clean operation. It produces oxygen and water as final products through the decomposition of residual ozone [102]. Ozone solubilizes sludge, decreasing biomass, resulting in a null of sludge generation [103,104].

Ozone (O_3) has a strong oxidation capacity (E = 2.07 V). It is composed of a weak single bond and a strong double bond that reacts effectively with various organic

and inorganic compounds [105]. The primary partial reactions of ozone in water are Equations (13) and (14) [106],

$$O_3 + 2H^+ + 2e^- \rightarrow O_2 + H_2O \quad (13)$$

$$O_3 + H_2O + e^- \rightarrow O_2 + 2OH^- \quad (14)$$

Ozone generation occurs through different processes, and the corona discharge method is the most used. This method uses an electrical discharge to separate oxygen molecules and form ozone. It involves electrodes where air is collected and passed through. While it can be expensive, its clear advantages make it an important study area such as water treatment [107].

Ozone can be used to oxidize organic pollutants in wastewater in two ways: (i) direct oxidation with molecular ozone [107] and (ii) by indirect reaction generating free radicals •OH [108,109]; these two reaction routes are shown in Figure 7. The selectivity and reaction rate of ozone are both significantly influenced by pH.

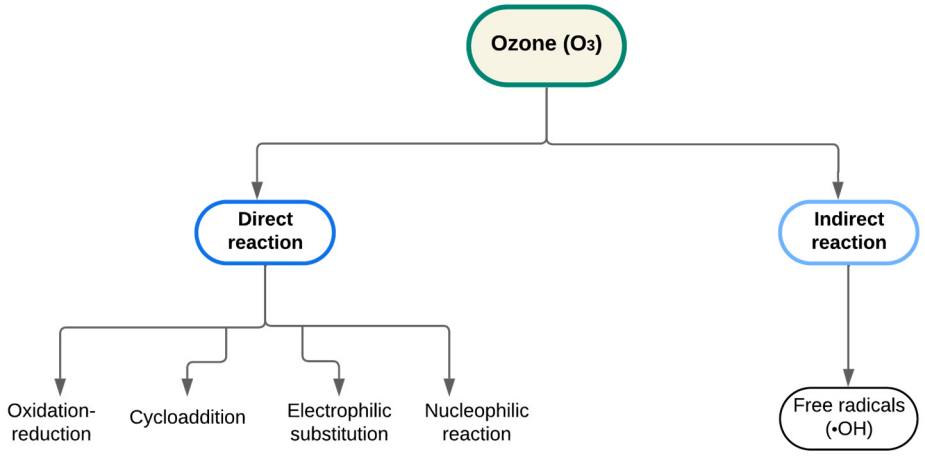

Figure 7. Schematic of the classification of the ozonation process.

The direct reaction, which typically occurs beneath acidic conditions (pH < 4), shows a high selectivity in attacking unsaturated bonds in organic compounds, but proceeds at a slow rate. Conversely, the indirect reaction under alkaline conditions (pH > 7) leads to rapid ozone decomposition and the generation of •OH radicals. This indirect reaction, while faster, is less selective with some compounds dissolved in water. Hydroxyl radicals (•OH), in the indirect ozonation mechanism, initiate a chain reaction that includes initiation, propagation, and termination. For an acidic-to-neutral pH, the indirect reactions start with the reaction in Equation (15) [103,110], while for an alkaline pH, ozone decomposes rapidly because the amount of hydroxyl ions (OH^-) in the solution increases, initiating chain reactions; the reactions involved are shown in Equations (16) and (17) [103,105]. From these reactions, hydroperoxyl ion (HO_2^-), superoxide anion $\left(O_2^-\right)$, and ozone anion ($O_3{}^-$) are produced [103,110]. The hydroperoxide ion plays a crucial role in this sequence, reacting rapidly to generate hydroperoxyl radical ($HO_2^\bullet$) [106], which can react again to obtain oxygen and hydroxyl radical (Equation (18)), or hydrogen peroxide (Equation (19)) [111],

$$O_3 + OH^- \rightarrow O_2^- + HO_2^\bullet \quad (15)$$

$$O_3 + OH^- \rightarrow HO_2^- + O_2 \quad (16)$$

$$O_3 + HO_2^- \rightarrow HO_2^\bullet + \left(\bullet O_3^-, \bullet O_2^-, \bullet OH\right) \quad (17)$$

$$O_3 + HO_2^{\bullet} \rightarrow 2O_2 + \bullet OH \quad (18)$$

$$2(HO_2^{\bullet}) \rightarrow O_2 + H_2O_2 \quad (19)$$

On the other hand, it has been observed that ozone alone does not achieve effective mineralization of recalcitrant organic pollutants in wastewater treatment. In addition, some works have reported that the chemical structure of compounds such as amines, ketones, binary, and ternary salts are not mineralized by ozone alone [112,113], so combining it with advanced oxidation processes, such as hydrogen peroxide and UV light are necessary.

Ozone-based AOPs can oxidize recalcitrant compounds in biodegradable products [114,115]. For this reason, more efficient ozonation processes integrate H_2O_2, UV radiation, and metal catalysts [116,117]. Catalytic ozonation can be classified as homogeneous or heterogeneous depending on the type of catalyst employed.

2.3.1. Homogeneous Catalytic Ozonation

This catalytic ozonation process improves the elimination of several organic contaminants from wastewater [118,119]. Various metal ions (Cr^{3+}, Mn^{2+}, Fe^{2+}, Ni^{2+}, Co^{2+}, Cu^{2+}, and Zn^{2+}) have been employed to remove recalcitrant organic pollutants by homogeneous catalytic ozonation [120,121]. However, water pollution from the use of metal ions is becoming an important problem [122,123]. To avoid these drawbacks and to increase the surface area, efficiency, and stability of the catalyst [124], these active species and metallic oxides have been immobilized on supports such as bentonite, sepiolite, montmorillonite, silica, and activated carbon [123,124].

2.3.2. Heterogeneous Catalytic Ozonation

This catalytic ozonation process promotes more efficient and faster oxidation reactions [125]. The advantages of heterogeneous catalytic ozonation include high stability and efficiency, complete mineralization of contaminants, no additional or secondary contamination, no need for a continuous supply of reagents, and the ability to reuse and regenerate the catalyst [126,127].

Various heterogeneous catalysts for ozonation have their own physicochemical and catalytic characteristics. Their greater surface area and more active sites allow for better catalytic performance [128], generally metal oxides are used as heterogeneous catalytic ozonation (Table 2). In addition, chemisorption reactions involving ozone, the catalytic surface, and organic compounds occur simultaneously [9].

Table 2. Summary of heterogeneous ozonation catalysts for the removal of organic pollutants in wastewater.

Organic Pollutants	Catalyst	Reaction Conditions	Remotion	Ref
Wastewater from yeast production	MnO_2	COD_o = 880 mg/L Catalyst loading = 6 g/L O_3 350 m/L pH = 12.0 Reaction time = 20 min	56.02%	[129]
Petroleum refinery wastewater	Mn-Fe-Cu/Al_2O_3	COD_o = 2825 mg/L Catalyst loading = 7 g/L O_3 2.9 g/h pH = 8.2 Reaction time = 60 min	67.1%	[42]

Table 2. *Cont.*

Organic Pollutants	Catalyst	Reaction Conditions	Remotion	Ref
Wastewater from paper production	Fe-NZ	COD_o = 400 mg/L Catalyst loading = 10 g/L O_3 300 m/L pH = 9.0 Reaction time = 120 min	71.01%	[130]
Organic wastewater (high salt content)	Ca-C/Al_2O_3	COD_o = 100–126 mg/L Catalyst loading = 400 g/L O_3 12 m/L pH = 8.36 Reaction time = 40 min	64.40%	[131]
Hypersaline wastewater	SnO_x-MnO_x/Al_2O_3	COD_o = 500 mg/L Catalyst loading = 40 g/L O_3 6 m/L pH = 7.0 Reaction time = 240 min	93.80%	[132]
Phenacetin (PNT)	$CuFe_2O_4$	$[PNT]_o$ = 0.2 mM Catalyst loading = 2 g/L O_3 0.36 m/L pH = 7.72 Reaction time = 180 min	70%	[133]
Sulfamethoxazole (SMX)	Fe_2O_3/CeO_2/Actived Carbon	$[SMX]_o$ = 40 mg/L Catalyst loading = 2 g/L O_3 48 mg/L pH = 7.5 Reaction time = 15 min	86%	[134]
Ibuprofen (IBU)	Fe_2O_3/Al_2O_3@SBA-15	$[IBU]_o$ = 10 mg/L Catalyst loading = 1.5 g/L O_3 30 m/L pH = 7.0 Reaction time = 60 min	90%	[135]
Reactive Black 5 dye (RB5)	Ag-Ce-O	$[RB5]_o$ = 100 mg/L Catalyst loading = 0.7 g/L O_3 60 L/h pH = 10.0 Reaction time = 80 min	88%	[136]
4-Chlorophenol (4-CP)	$MnFe_2O_4$	$[4\text{-}CP]_o$ = 100 mg/L Catalyst loading = 1 g/L O_3 5 mg/L pH = 6.21 Reaction time = 30 min	95.7%	[137]
Indigo carmine (IC)	Fe-pillared clay	$[IC]_o$ = 1000 mg/L Catalyst loading = 100 mg/L O_3 0.045 L/min pH = 3.0 Reaction time = 60 min	100%	[138]

According to the above results, heterogeneous catalysts can effectively remove various organic pollutants in wastewater by combining the oxidizing characteristics of ozone with the activity of catalysts [125]. Table 2 further illustrates the diversity in the pH range used, which underlines the importance of this parameter in the catalytic ozonation process and its impact on the degradation pathway. In the direct reaction, molecular ozone is transferred from the gaseous to the liquid phase, reacting with organic compounds, and in the indirect reaction, the ozone generates various radicals [139].

Ozonation with Fe-Pillared Clay

Pillared iron clays (Fe-PILC) have also been shown to be effective in degrading indigo carmine (IC) by ozonation [138].

Bernal et al. [138] reported that ozone combined with Fe-PILCs allowed the degradation of indigo carmine to isatine, which decreased by up to 72% in 60 min.

The interaction of ozone with iron-pillared clays can improve the generation of •OH radicals, according to Equations (20) and (21) [140],

$$Fe^{2+} + O_3 \rightarrow FeO^{2+} + O_2 \quad (20)$$

$$FeO^{2+} \overset{H_2O_2}{\rightarrow} Fe^{3+} + \bullet OH + OH^- \quad (21)$$

The iron species in the pillared clay may generate the ferrous species shown in Equation (22),

$$6H^+ + O_3 + FeO \rightarrow FeO^{2+} + 3H_2O \quad (22)$$

Through the following reaction (Equation (23)), ferrous ions (Fe^{2+}) can be obtained from ferric ions (Fe^{3+}),

$$Fe^{3+} + H_2O_2 \rightarrow Fe^{2+} + HO_2^{\bullet} + H^+ \quad (23)$$

Likewise, Bernal et al. [138] reported that no significant effect was observed on the ozonation rate by pure bentonite, but there was when Fe-PILCs were used. According to the above results, iron-pillared clays represent a viable option. When combined with ozone, they are capable of degrading and mineralizing recalcitrant contaminants such as indigo carmine present in wastewater.

2.4. Catalytic Wet Hydrogen Peroxide Oxidation Process

Catalytic wet oxidation of hydrogen peroxide (CWPO) is a promising advanced oxidation process that utilizes hydrogen peroxide as an oxidizing agent and a heterogeneous catalyst capable of degrading organic and inorganic compounds from wastewater under moderate pressure and temperature conditions [141,142]. This process is based on the decomposition of H_2O_2 on the surface of a catalyst to generate hydroxyl radicals (•OH) and hydroperoxide ($HO_2^{\bullet}$). In fact, the incorporation of H_2O_2 in heterogeneous catalysis favors a greater participation of the hydroxyl radicals present in the reaction environment [143].

Pillared aluminum or iron clays represent a viable option for CWPO because these materials combine their porosity with the activity of the active sites, as well as for its abundance, stability, and low cost [144]. Table 3 summarizes works using pillared clays with various metals, such as copper, iron, manganese, and platinum.

Table 3. Summary of pillared clays in CWPO for the degradation of organic pollutants in wastewater.

Organic Pollutants	Catalyst	Reaction Conditions	Remotion	Ref
Phenol compounds in coffee wastewater	Al/Fe-pillared bentonite	COD_o = 38,416 mg/L Catalyst loading = 4.10 g H_2O_2 = 0.17 mol/L Flow rate = 2 mL/h pH = 4.2 Reaction time = 96 h Temperature = 25 °C Eight reuse cycles	X_{phenol} = 62.4% Selectivity to CO_2 = 67.5%	[145]
Phenol	Fe-Silica pillared clay (SPC)	$[Phenol]_o$ = 500 mg/L Catalyst loading = 2 g/L H_2O_2 = 0.1 mol/L Flow rate = 2 mL/h pH = 3.7 Reaction time = 120 min Temperature = 30 °C Three reuse cycles	X_{phenol} = 99.5%	[146]
Tyrosol	Cu/Al-pillared clay	$[Tyrosol]_o$ = 3.6 mmol/L Catalyst loading = 1.0 g/L H_2O_2 = 0.068 M Flow rate = 30 mL/h pH = 5.6 Reaction time = 60 min Temperature = 25 °C	$X_{tyrosol}$ = 100%	[147]
Phenol	Al-Ce-Fe/bentonite	$[Phenol]_o$ = 47 ppm (5×10^{-4} M) Catalyst loading = 0.5 g H_2O_2 = stoichiometric amount pH = 3.7 Reaction time = 4 h Temperature = 25 °C	X_{phenol} = 100%	[148]
Organic matter in surface water	Al/Fe-pillared clay	$[DOC]_o$ = 7.0 mg/L Catalyst loading = 3.81 g/L H_2O_2 = 0.037 mg/mg C. mg Fe Flow rate = 0.56 cm^3/min pH = dependent on sampling location Reaction time = 4 h Temperature = dependent on sampling location	90%	[149]

The catalytic activity of pillared clays is due to the active sites (metals) located in the pillars that form it and in the structure of the clay sheets [54,55]. Notably, adding H_2O_2 significantly enhances the participation and formation of the hydroxyl radicals in the reaction medium. These radicals depend on the concentration of the catalyst and the reaction temperature and are produced by a redox process when hydrogen peroxide meets the catalyst [150], as shown in the following reactions (Equations (24)–(30)), where R-H is the organic pollutant:

$$Fe^{3+}_{(PILC)} + H_2O_2 \rightarrow Fe^{2+}_{(PILC)} + HO_2^{\bullet} + H^+ \quad (24)$$

$$Fe^{2+}_{(PILC)} + H_2O_2 \rightarrow Fe^{3+}_{(PILC)} + \bullet OH + OH^- \quad (25)$$

$$R - H + \bullet OH \rightarrow R\bullet + H_2O \quad (26)$$

$$R\bullet + O_2 \rightarrow ROO\bullet \quad (27)$$

$$ROO\bullet + R - H \rightarrow ROOH + R\bullet \quad (28)$$

$$ROOH + Fe^{2+}_{(PILC)} \rightarrow RO\bullet + Fe^{3+}_{(PILC)} + OH^- \quad (29)$$

$$ROOH + Fe^{3+}_{(PILC)} \rightarrow ROO\bullet + Fe^{2+}_{(PILC)} + H^+ \quad (30)$$

As Table 3 shows, Fe-PILCs with various metals (Cu, Ce, Al) are highly efficient in the catalytic wet oxidation hydrogen peroxide of aqueous effluents with various recalcitrant pollutants. In the case of copper–aluminium pillared clays, the oxidation state of aluminium is Al^{3+}. Therefore, the oxidation–reduction reaction between Al^{3+} and H_2O_2 cannot generate hydroxyl radicals, so other metals such as copper with different oxidation states (Cu^+ and Cu^{2+}) must be incorporated, which decompose directly with H_2O_2 and produce •OH radicals.

When pillared clays are used in CWPO, the reactions can be carried out under mild pressure and temperature conditions, which makes the process more feasible. In addition to presenting high stability and catalytic activity, their leaching is insignificant, probably due to their structure, making them potential catalysts for the degradation of organic compounds.

2.5. Photocatalysis

Photocatalysis is an advanced oxidation process employed to degrade organic pollutants at low concentrations in wastewater [151]. It is generally carried out at room pressure and temperature, and oxidizing compounds are not necessary to add to the reaction medium [152,153].

In the process of photocatalysis, photonic energy, such as ultraviolet radiation, visible light, or sunlight, is converted into chemical energy by photocatalysts, typically semiconductors like TiO_2, ZnO, ZnS, Fe_2O_3, GaP, MoS_2, CdS, CeO_2, AgCl, WO_3, ZrO_2, SnO_2, $BiVO_4$, BiOBr, CdS, SiO_2, and WS_2 [151,154,155]. When photons, with energy equal to or greater than the band gap of the material (BG), hit the photocatalyst, an electron (e^-) is excited from the valence band (VB) to the conduction band (CB), creating a hole (h^+) in the valence band. This process generates the electron–hole pair (e^-h^+), which will participate in the reduction and oxidation of organic pollutants until complete mineralization (H_2O and CO_2) or until obtaining low-toxicity species [156,157] (Figure 8).

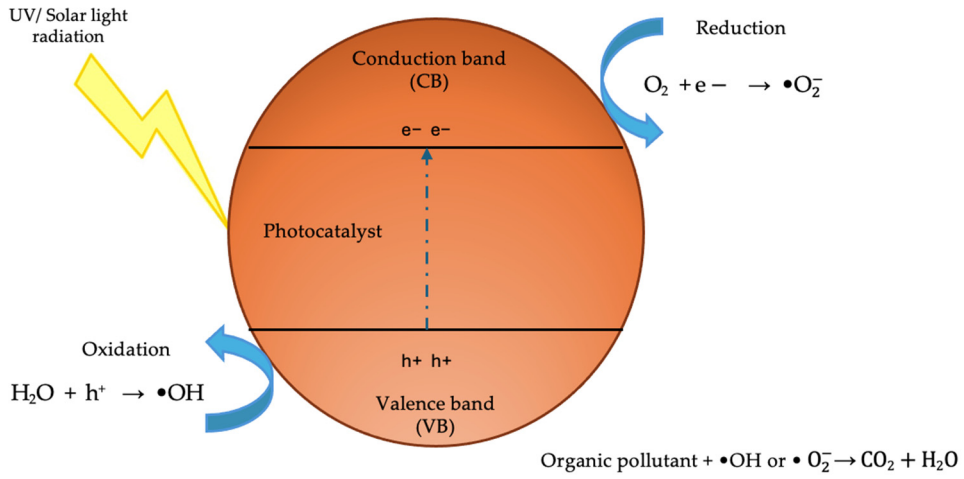

Figure 8. Schematic of photocatalysis reaction. Adapted with permission from [158]. Copyright 2024 Elsevier.

Chakravorty and Roy [154] reported that oxidation-reduction reactions take place on the surface of photocatalysts according to the following reactions (Equations (31)–(35)),

Photo excitation,

$$\text{Photocatlyst} + \text{hv} \rightarrow e^- + h^+ \quad (31)$$

Charge carrier trapping of e^-:

$$e^-_{CB} \rightarrow e^-_{TR} \quad (32)$$

Electron hole recombination:

$$e^-_{TR} + h^+_{VB}\left(h^+_{TR}\right) \rightarrow e^-_{CB} + \text{heat} \quad (33)$$

Oxidation of hydroxyls:

$$OH^- + h^+ \rightarrow \bullet OH \quad (34)$$

Photo-degradation of R-H (organic pollutant):

$$R - H + OH \rightarrow \bullet R' + H_2O \quad (35)$$

TiO_2 is among the most used photocatalysts since it presents an important difference between the valence (BV) and conduction (BC) bands, and its reaction generates a considerable oxidation power of the hydroxyl radical [154]. However, recent efforts have been made to develop photocatalysts with greater surface area and improve their catalytic activity in the visible region [159,160].

For this reason, various materials have been used as supports for TiO_2 or different photocatalysts to achieve their activity in visible light. Some of these materials are activated carbon [161], zeolites [162,163], silica [164,165], and clays [155,166]. These supports provide a high surface area, porosity, and easy recovery; in the case of titanium oxide, they prevent its aggregation [159].

Clays have been of the most important supports mentioned above because they are easy to obtain, relatively low cost, porous, chemically stable, non-toxic, and have high mechanical resistance [167,168]. Table 4 shows some works for the photocatalytic degradation of organic contaminants using pillared clays.

Table 4. Photocatalytic degradation of contaminants in wastewater using pillared clays.

Organic Pollutants	Photocatalyst	Reaction Conditions	Degradation	Ref
Metoprolol tartrate (MET)	TiO_2-FeAB (acidified bentonite) TiO_2/NB (natural bentonite)	[MET] = 3×10^{-5} M Catalyst loading = 1 g/L UV visible pH = 6.2 Temperature = 20 °C Reaction time = 300 min	80% 70%	[169]
Textile wastewater	TiO_2-anthill clay	[Textile wastewater] = 3.01 mg/L COD_o = 2.89 mg/L Catalyst loading = 2.05 wt% Sunlight pH = 2.0 Reaction time = 1.07 h Four cycles of reuse	70.92%	[170]

Table 4. *Cont.*

Organic Pollutants	Photocatalyst	Reaction Conditions	Degradation	Ref
Blue 19 dye	Nb_2O_5-bentonite	[Blue 19] = 30 mg/L Catalyst loading = 0.5 g 125 W mercury vapor lamp pH = 3.0 Reaction time = 2 h	98%	[171]
Acetaminophen	TiO_2-ZnO-cloisite clay	[ACE] = 10 mg/L Catalyst loading = 250 mg/L Solar light Reaction time = 10 h	100%	[172]
Phenol	Fe-TiO_2-Bentonite	[Phenol] = 5×10^{-4} M Catalyst loading = 0.5 g UV lamp (λ = 330–390 nm) pH = 3.7 Reaction time = 240 min	≅90%	[173]
Herbicides (bromacil, chlorotoluran and sulfosulfuron)	$TiOSO_4$-laponite	[Herbicides] = 5 ppm Catalyst loading = 50 mg UV radiation Reaction time = 60 min	80%	[174]
Solophenyl red 3BL (SR3BL)	TiO_2-pillared montmorillonite	[SR3BL] = 100 mg/L Catalyst loading = 2.5 g/L Solar radiation pH = 5.8 Reaction time = 220 min	95%	[175]
Rhodamine B (RHB) and tetracycline (TC)	g-C_3N_4-montmorillonite	[RHB] = 30 ppm [TC] = 100 ppm Catalyst loading = 2 g/L Visible light Reaction time = 360 min	87% (RhB) 76% (TC)	[176]
Tetracycline (TC)	NiO-montmorillonite	[TC] = 10 mg/L Catalyst loading = 0.8 g/L UV radiation (λ = 296 nm) Visible light pH = 6.8–7.1 Reaction time = 180 min Five cycles of use	94.2% (UV) 75.5% (Visible light)	[177]
2,4-dichlorophenoxyacetic acid (2,4-D)	Ti-pillared clay	[2,4-D] = 20 mg/L Catalyst loading = 120 mg (10.5 mmol of Ti/clay) UV radiation Reaction time = 90 min	≅70%	[178]
Acetaminophen (ACT)	Montmorillonite-Fe_2O_3/starch	[ACT] = 10 mg/L Catalyst loading = 0.75 g/L UVA radiation (λ = 365 nm) pH = 7.1 Reaction time = 80 min Four cycles of use	91%	[179]

Table 4. *Cont.*

Organic Pollutants	Photocatalyst	Reaction Conditions	Degradation	Ref
Trimethoprim (TMP)	Cr^{3+}/Ti-pillared clay montmorillonite	[TMP] = 25 mg/L Catalyst loading = 1 g/L UV radiation Reaction time = 180 min	76%	[180]
Triclosan (TCS)	TiO_2/Al-pillared clay	[TCS] = 90 µmol/L Catalyst loading = 1 g/L UV radiation pH = 4.0 Reaction time = 120 min	85.15 ± 0.49%	[181]
Methyl orange (MO)	TiO_2 pillared sericite	[MO] = 20 mg/L Catalyst loading = 50 mg UV radiation Reaction time = 80 min	98.5%	[182]

Table 4 shows that using various clays as supports for different semiconductors results in high percentages of degradation of organic contaminants using UV light, visible light, or sunlight. Therefore, it is demonstrated that pillared clays are viable for photocatalytic reactions to remove contaminants from water.

3. Future Perspectives

Pillared clays have been proven to play a crucial role in the generation of hydroxyl radicals, key species in advanced oxidation processes used to remove organic compounds in wastewater, so it is expected that these types of clays will continue to be useful for water recovery. Nevertheless, the application of pillared clays on advanced oxidation processes at industrial scale still faces a long road and some challenges to overcome. In this context, it is essential to implement more efficient synthesis methods and leave behind traditional approaches that demand large amounts of water for PILC production. This can significantly influence properties such as acidity, thermal stability, and porous structure, so it is important to optimize the process to make it more economically viable and decrease the environmental impacts without sacrificing efficiency.

It is also important to further extend the research on pillared clays and conduct lifecycle assessments to establish the environmental impacts of both, the catalyst synthesis and the wastewater treatment. In this sense, global warming potential, GWP (carbon footprint), is an environmental impact indicator that must be included in such studies. Within the advanced oxidation processes catalyzed by pillared clays, some of the stages affecting GWP are the activation of the catalyst through calcination and mixing during reaction, also energizing lamps used in photochemical processes by nonrenewable resources. Thus, it is of paramount importance to identify the active metal species required for the different advanced oxidation processes to optimize calcination temperatures and time, thus reducing the overall process's carbon footprint. In addition, and also in the context of processes activated by light, pillared clays with copper are promising because of their activity in the visible region of the electromagnetic spectrum.

Despite the great diversity of applications that clays have, there is practically no work that refers to immobilized clays, which would be very advantageous to avoid high-pressure drops when handling high volumes in the treatment of contaminated water. Some works have focused on the extrusion of honeycomb monoliths, but none on the immobilization of pillared clays on monoliths. The importance of these supports lies

in their use in bubble columns which, together with pillared clays, could intensify the advanced oxidation processes.

Finally, it is worth mentioning that by focusing on the application of pillared clays on oxidation processes, the chemical reduction implied in many cases has been generally overlooked, and this may become an important research line to convert pollutants like CO_2 into value-added compounds.

4. Conclusions

According to the report in this work, pillared clays demonstrate their potential as catalysts in advanced oxidation processes (Fenton, photo-Fenton, ozonation, catalytic peroxidation, and photocatalysis) intending to assist in the recovery and purification of wastewater from industrial, agricultural, hospital, and household sectors, with their treatment being crucial for achieving sustainable development.

The main lines of research focus on the use of pillared clays with different polyoxocations (Al, Fe, Zr, Mn, or Ti) or on the modification of clays with metals to optimize their catalytic activity or achieve the selective degradation of some contaminants, as well as allowing their use with UV light, visible light, or solar radiation.

Likewise, the use of pillared iron clays (Fe-PILCs) to remove a wide variety of organic contaminants, such as drugs, pesticides, dyes, and phenols from wastewater is shown.

In addition, pillared clays have several advantages that make them interesting, such as their porosity, stability, mechanical resistance, non-toxicity, easy recovery, and ability to work with pH values greater than 3.0, with minimal leaching of iron ions, maintaining their use in various reaction cycles. In most cases, complete mineralization of organic contaminants is achieved, or fewer contaminating intermediates are obtained.

Despite the above, pillared clays still have a long way to go to be used on an industrial scale. To achieve this, it is necessary to intensify the synthesis processes using, for example, ultrasound, the introduction of very specific polyoxocations to increase catalytic activity under visible light, and the identification of active species to optimize calcination temperatures and purification methods to achieve more sustainable and environmentally friendly processes.

Funding: This research was funded by Universidad Autónoma del Estado de México through Project 7058/2024CIB.

Data Availability Statement: Data will be provided upon request.

Acknowledgments: The technical support of Citlalit Martinez Soto and Elias Chavarria Rubio is also acknowledged.

Conflicts of Interest: The author declares no conflicts of interest.

References

1. OHCHR. 10th Anniversary of the Recognition of Water and Sanitation as a Human Right by the General Assembly. Available online: https://www.ohchr.org/en/statements/2020/07/10th-anniversary-recognition-water-and-sanitation-human-right-general-assembly (accessed on 25 July 2024).
2. UNICEF; World Health Organization (WHO). *Progress on Household Drinking-Water, Sanitation and Hygiene 2000–2022: Special Focus on Gender*; WHO: Geneva, Switzerland, 2023.
3. Crini, G.; Lichtfouse, E. Advantages and Disadvantages of Techniques Used for Wastewater Treatment. *Environ. Chem. Lett.* **2019**, *17*, 145–155. [CrossRef]
4. Rezai, B.; Allahkarami, E. *Wastewater Treatment Processes—Techniques, Technologies, Challenges Faced, and Alternative Solutions. Soft Computing Techniques Solid Waste Wastewater Management*; Elsevier: Amsterdam, The Netherlands, 2021; pp. 35–53. [CrossRef]
5. Vaz, T.; Quina, M.M.J.; Martins, R.C.; Gomes, J. Olive Mill Wastewater Treatment Strategies to Obtain Quality Water for Irrigation: A Review. *Sci. Total Environ.* **2024**, *931*, 172676. [CrossRef] [PubMed]

6. Fedorov, K.; Dinesh, K.; Sun, X.; Darvishi Cheshmeh Soltani, R.; Wang, Z.; Sonawane, S.; Boczkaj, G. Synergistic Effects of Hybrid Advanced Oxidation Processes (AOPs) Based on Hydrodynamic Cavitation Phenomenon—A Review. *Chem. Eng. J.* **2022**, *432*, 134191. [CrossRef]
7. Chai, W.S.; Cheun, J.Y.; Kumar, P.S.; Mubashir, M.; Majeed, Z.; Banat, F.; Ho, S.H.; Show, P.L. A Review on Conventional and Novel Materials towards Heavy Metal Adsorption in Wastewater Treatment Application. *J. Clean. Prod.* **2021**, *296*, 126589. [CrossRef]
8. Shabir, M.; Yasin, M.; Hussain, M.; Shafiq, I.; Akhter, P.; Nizami, A.S.; Jeon, B.H.; Park, Y.K. A Review on Recent Advances in the Treatment of Dye-Polluted Wastewater. *J. Ind. Eng. Chem.* **2022**, *112*, 1–19. [CrossRef]
9. Martínez-Huitle, C.A.; Rodrigo, M.A.; Sirés, I.; Scialdone, O. Single and Coupled Electrochemical Processes and Reactors for the Abatement of Organic Water Pollutants: A Critical Review. *Chem. Rev.* **2015**, *115*, 13362–13407. [CrossRef]
10. Hübner, U.; Spahr, S.; Lutze, H.; Wieland, A.; Rüting, S.; Gernjak, W.; Wenk, J. Advanced Oxidation Processes for Water and Wastewater Treatment—Guidance for Systematic Future Research. *Heliyon* **2024**, *10*, e30402. [CrossRef]
11. Zhou, A.; Du, J.; Zaoui, A.; Sekkal, W.; Sahimi, M. Molecular Modeling of Clay Minerals: A Thirty-Year Journey and Future Perspectives. *Coord. Chem. Rev.* **2025**, *526*, 216347. [CrossRef]
12. Das, S.; Prateek; Sharma, P.; Kumar, M.; Gupta, R.K.; Sharma, H. A Review on Clay Exfoliation Methods and Modifications for CO_2 Capture Application. *Mater. Today Sustain.* **2023**, *23*, 100427. [CrossRef]
13. Kloprogge, J.T. Synthesis of Smectites and Porous Pillared Clay Catalysts: A Review. *J. Porous Mater.* **1998**, *5*, 5–41. [CrossRef]
14. Li, J.; Sun, L.; Lv, G.; Liao, L. Application of Clay Minerals in Lithium-Sulfur Batteries: A Review. *J. Energy Storage* **2025**, *106*, 114852. [CrossRef]
15. Murray, H.H. Chapter 2 Structure and Composition of the Clay Minerals and Their Physical and Chemical Properties. *Dev. Clay Sci.* **2006**, *2*, 7–31. [CrossRef]
16. Najafi, H.; Farajfaed, S.; Zolgharnian, S.; Mosavi Mirak, S.H.; Asasian-Kolur, N.; Sharifian, S. A Comprehensive Study on Modified-Pillared Clays as an Adsorbent in Wastewater Treatment Processes. *Process Saf. Environ. Prot.* **2021**, *147*, 8–36. [CrossRef]
17. Cortés-Murillo, D.; Blanco-Jiménez, C.; Daza, C.E. Clay Exfoliation Method as a Route to Obtain Mesoporous Catalysts for CO_2 Methanation. *MethodsX* **2023**, *10*, 101955. [CrossRef]
18. Xu, Z.; Zhang, S.; Liu, J.; Xiao, Z.; Yang, M.; Tang, A. Kaolinite Nanoscroll Significantly Inhibiting Polysulfide Ions Shuttle in Lithium Sulfur Batteries. *Appl. Clay Sci.* **2022**, *224*, 106516. [CrossRef]
19. Moma, J.; Baloyi, J.; Ntho, T. Synthesis and Characterization of an Efficient and Stable Al/Fe Pillared Clay Catalyst for the Catalytic Wet Air Oxidation of Phenol. *RSC Adv.* **2018**, *8*, 30115–30124. [CrossRef]
20. Makó, É.; Kovács, A.; Kristóf, T. Influencing Parameters of Direct Homogenization Intercalation of Kaolinite with Urea, Dimethyl Sulfoxide, Formamide, and N-Methylformamide. *Appl. Clay Sci.* **2019**, *182*, 105287. [CrossRef]
21. Seifi, S.; Diatta-Dieme, M.T.; Blanchart, P.; Lecomte-Nana, G.L.; Kobor, D.; Petit, S. Kaolin Intercalated by Urea. Ceramic Applications. *Constr. Build. Mater.* **2016**, *113*, 579–585. [CrossRef]
22. Abdo, S.M.; El-Hout, S.I.; Shawky, A.; Rashed, M.N.; El-Sheikh, S.M. Visible-Light-Driven Photodegradation of Organic Pollutants by Simply Exfoliated Kaolinite Nanolayers with Enhanced Activity and Recyclability. *Environ. Res.* **2022**, *214*, 113960. [CrossRef]
23. Daza, C.E.; Gamba, O.A.; Hernández, Y.; Centeno, M.A.; Mondragón, F.; Moreno, S.; Molina, R. High-Stable Mesoporous Ni-Ce/Clay Catalysts for Syngas Production. *Catal. Lett.* **2011**, *141*, 1037–1046. [CrossRef]
24. Fazlali, F.; Mahjoub, A.R.; Aghayan, H. Adsorption of Toxic Heavy Metals onto Organofunctionalized Acid Activated Exfoliated Bentonite Clay for Achieving Wastewater Treatment Goals. *Desalination Water Treat.* **2019**, *152*, 338–350. [CrossRef]
25. Baloyi, J.; Ntho, T.; Moma, J. Synthesis and Application of Pillared Clay Heterogeneous Catalysts for Wastewater Treatment: A Review. *RSC Adv.* **2018**, *8*, 5197–5211. [CrossRef]
26. Litter, M.I. Introduction to Photochemical Advanced Oxidation Processes for Water Treatment. In *Environmental Photochemistry Part II*; Springer: Berlin/Heidelberg, Germany, 2005; pp. 325–366. [CrossRef]
27. Manna, M.; Sen, S. Advanced Oxidation Process: A Sustainable Technology for Treating Refractory Organic Compounds Present in Industrial Wastewater. *Environ. Sci. Pollut. Res. Int.* **2023**, *30*, 25477–25505. [CrossRef]
28. Saravanan, A.; Deivayanai, V.C.; Kumar, P.S.; Rangasamy, G.; Hemavathy, R.V.; Harshana, T.; Gayathri, N.; Alagumalai, K. A Detailed Review on Advanced Oxidation Process in Treatment of Wastewater: Mechanism, Challenges and Future Outlook. *Chemosphere* **2022**, *308*, 136524. [CrossRef]
29. Kokkinos, P.; Venieri, D.; Mantzavinos, D. Advanced Oxidation Processes for Water and Wastewater Viral Disinfection. A Systematic Review. *Food Environ. Virol.* **2021**, *13*, 283–302. [CrossRef] [PubMed]
30. Dobrosz-Gómez, I.; Quintero-Arias, J.D.; Gómez-García, M.Á. Fenton Advanced Oxidation Process for the Treatment of Industrial Textile Wastewater Highly Polluted with Acid-Black 194 Dye. *Case Stud. Chem. Environ. Eng.* **2024**, *9*, 100672. [CrossRef]
31. Rigg, T.; Taylor, W.; Weiss, J. The Rate Constant of the Reaction between Hydrogen Peroxide and Ferrous Ions. *J. Chem. Phys.* **1954**, *22*, 575–577. [CrossRef]
32. Walling, C.; Goosen, A. Mechanism of the Ferric Ion Catalyzed Decomposition of Hydrogen Peroxide. Effect of Organic Substrates. *J. Am. Chem. Soc.* **1973**, *95*, 2987–2991. [CrossRef]

33. Bielski, B.H.J.; Cabelli, D.E.; Arudi, R.L.; Ross, A.B. Reactivity of $HO_2/O-2$ Radicals in Aqueous Solution. *J. Phys. Chem. Ref. Data* **1985**, *14*, 1041–1100. [CrossRef]
34. Diya'uddeen, B.H.; Pouran, R.; Abdul Aziz, A.R.; Daud, W.M.A.W. Fenton Oxidative Treatment of Petroleum Refinery Wastewater: Process Optimization and Sludge Characterization. *RSC Adv.* **2015**, *5*, 68159–68168. [CrossRef]
35. Babuponnusami, A.; Muthukumar, K. A Review on Fenton and Improvements to the Fenton Process for Wastewater Treatment. *J. Environ. Chem. Eng.* **2014**, *2*, 557–572. [CrossRef]
36. Das, A.; Adak, M.K. Photo-Catalyst for Wastewater Treatment: A Review of Modified Fenton, and Their Reaction Kinetics. *Appl. Surf. Sci. Adv.* **2022**, *11*, 100282. [CrossRef]
37. Xu, X.R.; Li, X.Y.; Li, X.Z.; Li, H. Bin Degradation of Melatonin by UV, UV/H_2O_2, Fe^{2+}/H_2O_2 and UV/Fe^{2+}/H_2O_2 Processes. *Sep. Purif. Technol.* **2009**, *68*, 261–266. [CrossRef]
38. Xu, M.; Wu, C.; Zhou, Y.; Xu, M.; Wu, C.; Zhou, Y. Advancements in the Fenton Process for Wastewater Treatment. In *Advanced Oxidation Processes—Applications, Trends, and Prospects*; Intechopen: London, UK, 2020. [CrossRef]
39. Zhang, T.; Wen, Y.; Pan, Z.; Kuwahara, Y.; Mori, K.; Yamashita, H.; Zhao, Y.; Qian, X. Overcoming Acidic H_2O_2/Fe(II/III) Redox-Induced Low H_2O_2 Utilization Efficiency by Carbon Quantum Dots Fenton-like Catalysis. *Environ. Sci. Technol.* **2022**, *56*, 2617–2625. [CrossRef] [PubMed]
40. Poyatos, J.M.; Muñio, M.M.; Almecija, M.C.; Torres, J.C.; Hontoria, E.; Osorio, F. Advanced Oxidation Processes for Wastewater Treatment: State of the Art. *Water Air Soil Pollut.* **2010**, *205*, 187–204. [CrossRef]
41. Abril-González, M.; Seminario, D.; Pinos-Vélez, V.; Vele, A.; Echeverria-Paredes, P. An Activated Steel Scale Waste Catalyst to Degrade Methylene Blue via the Heterogeneous Fenton Process. *Case Stud. Chem. Environ. Eng.* **2024**, *10*, 100857. [CrossRef]
42. Wang, J.; Tang, J. Fe-Based Fenton-like Catalysts for Water Treatment: Preparation, Characterization and Modification. *Chemosphere* **2021**, *276*, 130177. [CrossRef] [PubMed]
43. Huang, W.; Wu, F.; Hanna, K.; Mailhot, G. Effect of Ethylenediamine-N,N′-Disuccinic Acid on Fenton and Photo-Fenton Processes Using Goethite as an Iron Source: Optimization of Parameters for Bisphenol A Degradation. *Environ. Sci. Pollut. Res.* **2013**, *20*, 39–50. [CrossRef] [PubMed]
44. He, J.; Yang, X.; Men, B.; Wang, D. Interfacial Mechanisms of Heterogeneous Fenton Reactions Catalyzed by Iron-Based Materials: A Review. *J. Environ. Sci.* **2016**, *39*, 97–109. [CrossRef] [PubMed]
45. Hussain, S.; Aneggi, E.; Goi, D. Catalytic Activity of Metals in Heterogeneous Fenton-like Oxidation of Wastewater Contaminants: A Review. *Environ. Chem. Lett.* **2021**, *19*, 2405–2424. [CrossRef]
46. Hasan, D.B.; Abdul Aziz, A.R.; Daud, W.M.A.W. Oxidative Mineralisation of Petroleum Refinery Effluent Using Fenton-like Process. *Chem. Eng. Res. Des.* **2012**, *90*, 298–307. [CrossRef]
47. Pergher, S.B.C.; Corma, A.; Fornes, V. Materiales Laminares Pilareados: Preparación y Propiedades. *Quim. Nova* **1999**, *22*, 693–709. [CrossRef]
48. Pandey, P.; Saini, V.K. Pillared Interlayered Clays: Sustainable Materials for Pollution Abatement. *Environ. Chem. Lett.* **2019**, *17*, 721–727. [CrossRef]
49. Gil, A.; Korili, S.A.; Trujillano, R.; Vicente, M.A. *Pillared Clays and Related Catalysts*; Springer: Berlin/Heidelberg, Germany, 2010; pp. 1–522. [CrossRef]
50. Hadj Bachir, D.; Khalaf, H.; Ferroukhi, S.; Boutoumi, Y.; Schnee, J.; Gaigneaux, E.M. Preparation and Characterization of TiO_2 Pillared Clay: Effect of Palladium and Photosensitizer on Photocatalytic Activity. *Res. J. Chem. Environ.* **2020**, *24*, 60–73.
51. Cardona, Y.; Korili, S.A.; Gil, A. Use of Clays and Pillared Clays in the Catalytic Photodegradation of Organic Compounds in Aqueous Solutions. *Catal. Rev.* **2023**, *66*, 2063–2110. [CrossRef]
52. Zamisa, M.K.; Seadira, T.W.; Baloyi, S.J. Transforming Wastewater Treatment: Recent Advancements in Catalytic Wet Air Oxidation with Pillared Clay Catalysts for Phenol Remediation. *Environ. Pollut.* **2024**, *361*, 124842. [CrossRef] [PubMed]
53. Bobu, M.; Yediler, A.; Siminiceanu, I.; Schulte-Hostede, S. Degradation Studies of Ciprofloxacin on a Pillared Iron Catalyst. *Appl. Catal. B Environ.* **2008**, *83*, 15–23. [CrossRef]
54. Adams, J.M.; McCabe, R.W. Chapter 10.2 Clay Minerals as Catalysts. *Dev. Clay Sci.* **2006**, *1*, 541–581. [CrossRef]
55. Yurdakoç, M.; Akçay, M.; Tonbul, Y.; Ok, F.; Yurdakoç, K. Preparation and Characterization of Cr- and Fe-Pillared Bentonites by Using $CrCl_3$, $FeCl_3$, $Cr(Acac)_3$ and $Fe(Acac)_3$ as Precursors. *Microporous Mesoporous Mater.* **2008**, *111*, 211–218. [CrossRef]
56. Mokaya, R.; Jones, W. Pillared Clays and Pillared Acid-Activated Clays: A Comparative-Study of Physical, Acidic, and Catalytic Properties. *J. Catal.* **1995**, *153*, 76–85. [CrossRef]
57. Valverde, J.L.; Romero, A.; Romero, R.; García, P.B.; Sánchez, M.L.; Asencio, I. Preparation and Characterization of Fe-PILCS. Influence of the Synthesis Parameters. *Clays Clay Miner.* **2005**, *53*, 613–621. [CrossRef]
58. Hurtado, L.; Romero, R.; Mendoza, A.; Brewer, S.; Donkor, K.; Gómez-Espinosa, R.M.; Natividad, R. Paracetamol Mineralization by Photo Fenton Process Catalyzed by a Cu/Fe-PILC under Circumneutral PH Conditions. *J. Photochem. Photobiol. A Chem.* **2019**, *373*, 162–170. [CrossRef]

59. Mendoza, A.; Romero, R.; Gutiérrez-Cedillo, G.P.; López-Tellez, G.; Lorenzo-González, O.; Gómez-Espinosa, R.M.; Natividad, R. Selective Production of Dihydroxyacetone and Glyceraldehyde by Photo-Assisted Oxidation of Glycerol. *Catal. Today* **2020**, *358*, 149–154. [CrossRef]
60. Zhang, Y.; Hu, S.; Mi, X.; Zhang, R.; Sun, R.; Wu, Y. Nitrobenzene Removal by Novel Pillared Kaolinite-Catalyzed Fenton-like Reaction. *Desalination Water Treat.* **2021**, *218*, 210–219. [CrossRef]
61. Farhadirad, M.; Najafi, H.; Sharifian, S.; Ebrahimian Pirbazari, A.; Asasian-Kolur, N.; Harasek, M. Enhanced Levofloxacin Degradation through Fenton-like Process Using Fe-Silica Pillared Clay Catalyst. *Appl. Catal. O Open* **2024**, *190*, 206931. [CrossRef]
62. Khankhasaeva, S.T.; Dambueva, D.V.; Dashinamzhilova, E.T.; Gil, A.; Vicente, M.A.; Timofeeva, M.N. Fenton Degradation of Sulfanilamide in the Presence of Al,Fe-Pillared Clay: Catalytic Behavior and Identification of the Intermediates. *J. Hazard. Mater.* **2015**, *293*, 21–29. [CrossRef] [PubMed]
63. Tabet, D.; Saidi, M.; Houari, M.; Pichat, P.; Khalaf, H. Fe-Pillared Clay as a Fenton-Type Heterogeneous Catalyst for Cinnamic Acid Degradation. *J. Environ. Manag.* **2006**, *80*, 342–346. [CrossRef]
64. Boukhemkhem, A.; Bedia, J.; Belver, C.; Molina, C.B. Degradation of Pesticides by Heterogeneous Fenton Using Iron-Exchanged Clays. *Catal. Commun.* **2023**, *183*, 106771. [CrossRef]
65. Azmi, N.H.M.; Vadivelu, V.M.; Hameed, B.H. Iron-Clay as a Reusable Heterogeneous Fenton-like Catalyst for Decolorization of Acid Green 25. *Desalination Water Treat.* **2014**, *52*, 5583–5593. [CrossRef]
66. Ramirez, J.H.; Costa, C.A.; Madeira, L.M.; Mata, G.; Vicente, M.A.; Rojas-Cervantes, M.L.; López-Peinado, A.J.; Martín-Aranda, R.M. Fenton-like Oxidation of Orange II Solutions Using Heterogeneous Catalysts Based on Saponite Clay. *Appl. Catal. B Environ.* **2007**, *71*, 44–56. [CrossRef]
67. Feng, J.; Hu, X.; Yue, P.L.; Zhu, H.Y.; Lu, G.Q. A Novel Laponite Clay-Based Fe Nanocomposite and Its Photo-Catalytic Activity in Photo-Assisted Degradation of Orange II. *Chem. Eng. Sci.* **2003**, *58*, 679–685. [CrossRef]
68. Tatibouët, J.M.; Guélou, E.; Fournier, J. Catalytic Oxidation of Phenol by Hydrogen Peroxide over a Pillared Clay Containing Iron. Active Species and PH Effect. *Top. Catal.* **2005**, *33*, 225–232. [CrossRef]
69. Catrinescu, C.; Arsene, D.; Apopei, P.; Teodosiu, C. Degradation of 4-Chlorophenol from Wastewater through Heterogeneous Fenton and Photo-Fenton Process, Catalyzed by Al–Fe PILC. *Appl. Clay Sci.* **2012**, *58*, 96–101. [CrossRef]
70. De León, M.A.; Rodríguez, M.; Marchetti, S.G.; Sapag, K.; Faccio, R.; Sergio, M.; Bussi, J. Raw Montmorillonite Modified with Iron for Photo-Fenton Processes: Influence of Iron Content on Textural, Structural and Catalytic Properties. *J. Environ. Chem. Eng.* **2017**, *5*, 4742–4750. [CrossRef]
71. de Almeida, L.N.B.; Josué, T.G.; Fidelis, M.Z.; Abreu, E.; Bechlin, M.A.; dos Santos, O.A.A.; Lenzi, G.G. Process Comparison for Caffeine Degradation: Fenton, Photo-Fenton, UV/H_2O_2 and UV/Fe^{3+}. *Water Air Soil Pollut.* **2021**, *232*, 147. [CrossRef]
72. De León, M.A.; Castiglioni, J.; Bussi, J.; Sergio, M. Catalytic Activity of an Iron-Pillared Montmorillonitic Clay Mineral in Heterogeneous Photo-Fenton Process. *Catal. Today* **2008**, *133–135*, 600–605. [CrossRef]
73. Minella, M.; Marchetti, G.; De Laurentiis, E.; Malandrino, M.; Maurino, V.; Minero, C.; Vione, D.; Hanna, K. Photo-Fenton Oxidation of Phenol with Magnetite as Iron Source. *Appl. Catal B Environ.* **2014**, *154–155*, 102–109. [CrossRef]
74. Najjar, W.; Azabou, S.; Sayadi, S.; Ghorbel, A. Catalytic Wet Peroxide Photo-Oxidation of Phenolic Olive Oil Mill Wastewater Contaminants: Part I. Reactivity of Tyrosol over (Al–Fe)PILC. *Appl. Catal. B Environ.* **2007**, *74*, 11–18. [CrossRef]
75. Chen, J.; Zhu, L. Comparative Study of Catalytic Activity of Different Fe-Pillared Bentonites in the Presence of UV Light and H_2O_2. *Sep. Purif. Technol.* **2009**, *67*, 282–288. [CrossRef]
76. Soon, A.N.; Hameed, B.H. Heterogeneous Catalytic Treatment of Synthetic Dyes in Aqueous Media Using Fenton and Photo-Assisted Fenton Process. *Desalination* **2011**, *269*, 1–16. [CrossRef]
77. Nidheesh, P.V. Heterogeneous Fenton Catalysts for the Abatement of Organic Pollutants from Aqueous Solution: A Review. *RSC Adv.* **2015**, *5*, 40552–40577. [CrossRef]
78. Sum, O.S.N.; Feng, J.; Hu, X.; Yue, P.L. Pillared Laponite Clay-Based Fe Nanocomposites as Heterogeneous Catalysts for Photo-Fenton Degradation of Acid Black 1. *Chem. Eng. Sci.* **2004**, *59*, 5269–5275. [CrossRef]
79. Li, H.; Li, Y.; Xiang, L.; Huang, Q.; Qiu, J.; Zhang, H.; Sivaiah, M.V.; Baron, F.; Barrault, J.; Petit, S.; et al. Heterogeneous Photo-Fenton Decolorization of Orange II over Al-Pillared Fe-Smectite: Response Surface Approach, Degradation Pathway, and Toxicity Evaluation. *J. Hazard. Mater.* **2015**, *287*, 32–41. [CrossRef] [PubMed]
80. Sharma, G.; Tak, P.; Ameta, R.; Punjabi, P.B.; Sharma, S. Degradation of Methylene Blue Using Fe-Pillared Bentonite Clay. *Acta Chim. Pharm. Indica* **2015**, *5*, 8–15.
81. Bel Hadjltaief, H.; Da Costa, P.; Galvez, M.E.; Ben Zina, M. Influence of Operational Parameters in the Heterogeneous Photo-Fenton Discoloration of Wastewaters in the Presence of an Iron-Pillared Clay. *Ind. Eng. Chem. Res.* **2013**, *52*, 16656–16665. [CrossRef]
82. Bel Hadjltaief, H.; Da Costa, P.; Beaunier, P.; Gálvez, M.E.; Ben Zina, M. Fe-Clay-Plate as a Heterogeneous Catalyst in Photo-Fenton Oxidation of Phenol as Probe Molecule for Water Treatment. *Appl. Clay Sci.* **2014**, *91–92*, 46–54. [CrossRef]

83. Herney-Ramirez, J.; Vicente, M.A.; Madeira, L.M. Heterogeneous Photo-Fenton Oxidation with Pillared Clay-Based Catalysts for Wastewater Treatment: A Review. *Appl. Catal B Environ.* **2010**, *98*, 10–26. [CrossRef]
84. Mèçabih, Z. Fe-Al-Pillared Clay Used for Conversion of Toluene Through Catalytic Wet Peroxide Oxidation. *Pet. Sci. Eng.* **2018**, *2*, 17–24. [CrossRef]
85. Bracco, E.B.; Marco-Brown, J.L.; Butler, M.; Candal, R.J. Degradation of Oxytetracycline and Characterization of Byproducts Generated by Fenton or Photo-Fenton like Processes after Adsorption on Natural and Iron(III)-Modified Montmorillonite Clays. *Environ. Nanotechnol. Monit. Manag.* **2023**, *19*, 100778. [CrossRef]
86. Sum, O.S.N.; Feng, J.; Hu, X.; Yue, P.L. Photo-Assisted Fenton Mineralization of an Azo-Dye Acid Black 1 Using a Modified Laponite Clay-Based Fe Nanocomposite as a Heterogeneous Catalyst. *Top. Catal.* **2005**, *33*, 233–242. [CrossRef]
87. Feng, J.; Hu, X.; Yue, P.L. Effect of Initial Solution PH on the Degradation of Orange II Using Clay-Based Fe Nanocomposites as Heterogeneous Photo-Fenton Catalyst. *Water Res.* **2006**, *40*, 641–646. [CrossRef] [PubMed]
88. Guo, S.; Yang, W.; You, L.; Li, J.; Chen, J.; Zhou, K. Simultaneous Reduction of Cr(VI) and Degradation of Tetracycline Hydrochloride by a Novel Iron-Modified Rectorite Composite through Heterogeneous Photo-Fenton Processes. *Chem. Eng. J.* **2020**, *393*, 124758. [CrossRef]
89. Meijide, J.; Lama, G.; Pazos, M.; Sanromán, M.A.; Dunlop, P.S.M. Ultraviolet-Based Heterogeneous Advanced Oxidation Processes as Technologies to Remove Pharmaceuticals from Wastewater: An Overview. *J. Environ. Chem. Eng.* **2022**, *10*, 107630. [CrossRef]
90. Bueno, N.; Pérez, A.; Molina, R.; Moreno, S. Pillared Bentonite from Al-Fe-Cu Polymeric Precursor in Solid State for the Catalytic Oxidation of Amoxicillin. *Catal. Today* **2023**, *418*, 114135. [CrossRef]
91. Khelifi, S.; Ayari, F. Modified Bentonite for Anionic Dye Removal from Aqueous Solutions. Adsorbent Regeneration by the Photo-Fenton Process. *C. R. Chim.* **2019**, *22*, 154–160. [CrossRef]
92. Liu, Z.; Zhang, Y.; Lee, J.; Xing, L. A Review of Application Mechanism and Research Progress of Fe/Montmorillonite-Based Catalysts in Heterogeneous Fenton Reactions. *J. Environ. Chem. Eng.* **2024**, *12*, 112152. [CrossRef]
93. Molina, C.B.; Sanz-Santos, E.; Boukhemkhem, A.; Bedia, J.; Belver, C.; Rodriguez, J.J. Removal of Emerging Pollutants in Aqueous Phase by Heterogeneous Fenton and Photo-Fenton with Fe_2O_3-TiO_2-Clay Heterostructures. *Environ. Sci. Pollut. Res.* **2020**, *27*, 38434–38445. [CrossRef] [PubMed]
94. Hadjltaief, H.B.; Zina, M.B.; Galvez, M.E.; Da Costa, P. Photo-Fenton Oxidation of Phenol over a Cu-Doped Fe-Pillared Clay. *C. R. Chim.* **2015**, *18*, 1161–1169. [CrossRef]
95. Bosio, G.N.; García Einschlag, F.S.; Carlos, L.; Mártire, D.O. Recent Advances in the Development of Novel Iron–Copper Bimetallic Photo Fenton Catalysts. *Catalysts* **2023**, *13*, 159. [CrossRef]
96. Navalon, S.; Alvaro, M.; Garcia, H. Heterogeneous Fenton Catalysts Based on Clays, Silicas and Zeolites. *Appl. Catal. B Environ.* **2010**, *99*, 1–26. [CrossRef]
97. Timofeeva, M.N.; Khankhasaeva, S.T.; Talsi, E.P.; Panchenko, V.N.; Golovin, A.V.; Dashinamzhilova, E.T.; Tsybulya, S.V. The Effect of Fe/Cu Ratio in the Synthesis of Mixed Fe,Cu,Al-Clays Used as Catalysts in Phenol Peroxide Oxidation. *Appl. Catal. B Environ.* **2009**, *90*, 618–627. [CrossRef]
98. Dorado, F.; de Lucas, A.; García, P.B.; Valverde, J.L.; Romero, A. Preparation of Cu-Ion-Exchanged Fe-PILCs for the SCR of NO by Propene. *Appl. Catal. B Environ.* **2006**, *65*, 175–184. [CrossRef]
99. Sun, Y.; Yang, Z.; Tian, P.; Sheng, Y.; Xu, J.; Han, Y.F. Oxidative Degradation of Nitrobenzene by a Fenton-like Reaction with Fe-Cu Bimetallic Catalysts. *Appl. Catal. B Environ.* **2019**, *244*, 1–10. [CrossRef]
100. Wei, Y.; Wang, C.; Liu, D.; Jiang, L.; Chen, X.; Li, H.; Zhang, F. Photo-Catalytic Oxidation for Pyridine in Circumneutral Aqueous Solution by Magnetic Fe-Cu Materials Activated H_2O_2. *Chem. Eng. Res. Des.* **2020**, *163*, 1–11. [CrossRef]
101. Zhang, Y.; Fan, J.; Yang, B.; Huang, W.; Ma, L. Copper–Catalyzed Activation of Molecular Oxygen for Oxidative Destruction of Acetaminophen: The Mechanism and Superoxide-Mediated Cycling of Copper Species. *Chemosphere* **2017**, *166*, 89–95. [CrossRef]
102. Rekhate, C.V.; Srivastava, J.K. Recent Advances in Ozone-Based Advanced Oxidation Processes for Treatment of Wastewater—A Review. *Chem. Eng. J. Adv.* **2020**, *3*, 100031. [CrossRef]
103. Joseph, C.G.; Farm, Y.Y.; Taufiq-Yap, Y.H.; Pang, C.K.; Nga, J.L.H.; Li Puma, G. Ozonation Treatment Processes for the Remediation of Detergent Wastewater: A Comprehensive Review. *J. Environ. Chem. Eng.* **2021**, *9*, 106099. [CrossRef]
104. Lim, S.; Shi, J.L.; von Gunten, U.; McCurry, D.L. Ozonation of Organic Compounds in Water and Wastewater: A Critical Review. *Water Res.* **2022**, *213*, 118053. [CrossRef] [PubMed]
105. Chandrasekara Pillai, K.; Kwon, T.O.; Moon, I.S. Degradation of Wastewater from Terephthalic Acid Manufacturing Process by Ozonation Catalyzed with Fe^{2+}, H_2O_2 and UV Light: Direct versus Indirect Ozonation Reactions. *Appl. Catal. B Environ.* **2009**, *91*, 319–328. [CrossRef]
106. Ikehata, K.; Li, Y. Ozone-Based Processes. In *Advanced Oxidation Processes for Wastewater Treatment: Emerging Green Chemical Technology*; Academic Press: New York, NY, USA, 2018; pp. 115–134. [CrossRef]
107. Das, P.P.; Dhara, S.; Samanta, N.S.; Purkait, M.K. Advancements on Ozonation Process for Wastewater Treatment: A Comprehensive Review. *Chem. Eng. Process.—Process Intensif.* **2024**, *202*, 109852. [CrossRef]

108. Guinea, E.; Brillas, E.; Centellas, F.; Cañizares, P.; Rodrigo, M.A.; Sáez, C. Oxidation of Enrofloxacin with Conductive-Diamond Electrochemical Oxidation, Ozonation and Fenton Oxidation. A Comparison. *Water Res.* **2009**, *43*, 2131–2138. [CrossRef] [PubMed]
109. Liu, Z.; Demeestere, K.; Hulle, S. Van Comparison and Performance Assessment of Ozone-Based AOPs in View of Trace Organic Contaminants Abatement in Water and Wastewater: A Review. *J. Environ. Chem. Eng.* **2021**, *9*, 105599. [CrossRef]
110. Liang, J.; Fei, Y.; Yin, Y.; Han, Q.; Liu, Y.; Feng, L.; Zhang, L. Advancements in Wastewater Treatment: A Comprehensive Review of Ozone Microbubbles Technology. *Environ. Res.* **2025**, *266*, 120469. [CrossRef] [PubMed]
111. Hernández-Ortega, M.; Ponziak, T.; Barrera-Díaz, C.; Rodrigo, M.A.; Roa-Morales, G.; Bilyeu, B. Use of a Combined Electrocoagulation–Ozone Process as a Pre-Treatment for Industrial Wastewater. *Desalination* **2010**, *250*, 144–149. [CrossRef]
112. Hoigné, J.; Bader, H. Rate Constants of Reactions of Ozone with Organic and Inorganic Compounds in Water—I: Non-Dissociating Organic Compounds. *Water Res.* **1983**, *17*, 173–183. [CrossRef]
113. Sreethawong, T.; Chavadej, S. Color Removal of Distillery Wastewater by Ozonation in the Absence and Presence of Immobilized Iron Oxide Catalyst. *J. Hazard. Mater.* **2008**, *155*, 486–493. [CrossRef] [PubMed]
114. Lee, B.H.; Song, W.C.; Manna, B.; Ha, J.K. Dissolved Ozone Flotation (DOF)—A Promising Technology in Municipal Wastewater Treatment. *Desalination* **2008**, *225*, 260–273. [CrossRef]
115. Rosal, R.; Rodríguez, A.; Perdigón-Melón, J.A.; Petre, A.; García-Calvo, E.; Rosal, R.; Rodríguez, A.; Perdigón-Melón, J.A.; Petre, A.; García-Calvo, E. Oxidation of Dissolved Organic Matter in the Effluent of a Sewage Treatment Plant Using Ozone Combined with Hydrogen Peroxide (O_3/H_2O_2). *Chem. Eng. J.* **2009**, *149*, 311–318. [CrossRef]
116. Nieto-Sandoval, J.; Ammar, R.; Sans, C. Enhancing Nanoplastics Removal by Metal Ion-Catalyzed Ozonation. *Chem. Eng. J. Adv.* **2024**, *19*, 100621. [CrossRef]
117. Ziwei, Y.; Zhe, W.; Shaopo, W.; Jingjie, Y.; Chen, L.; Jing, C. Mechanism of Ozone Catalysis by Transition Metal Hydroxyl Oxides: From Reactive Oxygen Species to Surface Structural Hydroxyl. *Desalination Water Treat.* **2024**, *320*, 100823. [CrossRef]
118. Li, X.; Ma, J.; He, H. Recent Advances in Catalytic Decomposition of Ozone. *J. Environ. Sci.* **2020**, *94*, 14–31. [CrossRef] [PubMed]
119. Fu, P.; Wang, L.; Li, G.; Hou, Z.; Ma, Y. Homogenous Catalytic Ozonation of Aniline Aerofloat Collector by Coexisted Transition Metallic Ions in Flotation Wastewaters. *J. Environ. Chem. Eng.* **2020**, *8*, 103714. [CrossRef]
120. Wu, C.H.; Kuo, C.Y.; Chang, C.L. Homogeneous Catalytic Ozonation of C.I. Reactive Red 2 by Metallic Ions in a Bubble Column Reactor. *J. Hazard. Mater.* **2008**, *154*, 748–755. [CrossRef]
121. Zhang, Z.; Xiang, L.; Lin, F.; Wang, Z.; Yan, B.; Chen, G. Catalytic Deep Degradation of Cl-VOCs with the Assistance of Ozone at Low Temperature over MnO_2 Catalysts. *Chem. Eng. J.* **2021**, *426*, 130814. [CrossRef]
122. Pachhade, K.; Sandhya, S.; Swaminathan, K. Ozonation of Reactive Dye, Procion Red MX-5B Catalyzed by Metal Ions. *J. Hazard. Mater.* **2009**, *167*, 313–318. [CrossRef] [PubMed]
123. Gu, L.; Zhang, X.; Lei, L. Degradation of Aqueous P-Nitrophenol by Ozonation Integrated with Activated Carbon. *Ind. Eng. Chem. Res.* **2008**, *47*, 6809–6815. [CrossRef]
124. Feng, C.; Zhao, J.; Qin, G.; Diao, P. Construction of the Fe^{3+}-O-$Mn^{3+/2+}$ Hybrid Bonds on the Surface of Porous Silica as Active Centers for Efficient Heterogeneous Catalytic Ozonation. *J. Solid State Chem.* **2021**, *300*, 122266. [CrossRef]
125. Issaka, E.; Baffoe, J.; Adams, M. Exploring Heterogeneous Catalytic Ozonation: Catalyst Types, Reaction Mechanisms, Applications, Challenges, and Future Outlook. *Sustain. Chem. Environ.* **2024**, *8*, 100185. [CrossRef]
126. Issaka, E.; Amu-Darko, J.N.O.; Yakubu, S.; Fapohunda, F.O.; Ali, N.; Bilal, M. Advanced Catalytic Ozonation for Degradation of Pharmaceutical Pollutants—A Review. *Chemosphere* **2022**, *289*, 133208. [CrossRef]
127. Khuntia, S.; Majumder, S.K.; Ghosh, P. Catalytic Ozonation of Dye in a Microbubble System: Hydroxyl Radical Contribution and Effect of Salt. *J. Environ. Chem. Eng.* **2016**, *4*, 2250–2258. [CrossRef]
128. Zhang, R.; Jin, H.; Ma, L.; Yang, S.; He, G. Synergistic Catalytic Performance of RuSn and PdCe Composite Catalysts for the Hydrogenation of Terephthalic Acid to 1,4-Cyclohexanedimethanol. *Catal. Commun.* **2024**, *187*, 106887. [CrossRef]
129. Jing, X.; Cheng, S.; Men, C.; Zhu, H.; Luo, M.; Li, Z. Study on the Mechanism and Control Strategy of Advanced Treatment of Yeast Wastewater by Ozone Catalytic Oxidation. *Water* **2023**, *15*, 274. [CrossRef]
130. Munir, H.M.S.; Feroze, N.; Ramzan, N.; Sagir, M.; Babar, M.; Tahir, M.S.; Shamshad, J.; Mubashir, M.; Khoo, K.S. Fe-Zeolite Catalyst for Ozonation of Pulp and Paper Wastewater for Sustainable Water Resources. *Chemosphere* **2022**, *297*, 134031. [CrossRef] [PubMed]
131. Chen, J.; Tu, Y.; Shao, G.; Zhang, F.; Zhou, Z.; Tian, S.; Ren, Z. Catalytic Ozonation Performance of Calcium-Loaded Catalyst (Ca-C/Al_2O_3) for Effective Treatment of High Salt Organic Wastewater. *Sep. Purif. Technol.* **2022**, *301*, 121937. [CrossRef]
132. Guo, H.; Li, X.; Li, G.; Liu, Y.; Rao, P. Preparation of SnO_x-MnO_x@Al_2O_3 for Catalytic Ozonation of Phenol in Hypersaline Wastewater. *Ozone Sci. Eng.* **2023**, *45*, 262–275. [CrossRef]
133. Qi, F.; Chu, W.; Xu, B. Ozonation of Phenacetin in Associated with a Magnetic Catalyst $CuFe_2O_4$: The Reaction and Transformation. *Chem. Eng. J.* **2015**, *262*, 552–562. [CrossRef]

134. Akhtar, J.; Amin, N.A.S.; Aris, A. Combined Adsorption and Catalytic Ozonation for Removal of Sulfamethoxazole Using Fe_2O_3/CeO_2 Loaded Activated Carbon. *Chem. Eng. J.* **2011**, *170*, 136–144. [CrossRef]
135. Bing, J.; Hu, C.; Nie, Y.; Yang, M.; Qu, J. Mechanism of Catalytic Ozonation in Fe_2O_3/Al_2O_3@SBA-15 Aqueous Suspension for Destruction of Ibuprofen. *Environ. Sci. Technol.* **2015**, *49*, 1690–1697. [CrossRef]
136. Chokshi, N.P.; Chauhan, A.; Chhayani, R.; Sharma, S.; Ruparelia, J.P. Preparation and Application of Ag–Ce–O Composite Metal Oxide Catalyst in Catalytic Ozonation for Elimination of Reactive Black 5 Dye from Aqueous Media. *Water Sci. Eng.* **2024**, *17*, 257–265. [CrossRef]
137. Chen, J.; Wen, W.; Kong, L.; Tian, S.; Ding, F.; Xiong, Y. Magnetically Separable and Durable $MnFe_2O_4$ for Efficient Catalytic Ozonation of Organic Pollutants. *Ind. Eng. Chem. Res.* **2014**, *53*, 6297–6306. [CrossRef]
138. Bernal, M.; Romero, R.; Roa, G.; Barrera-Díaz, C.; Torres-Blancas, T.; Natividad, R. Ozonation of Indigo Carmine Catalyzed with Fe-Pillared Clay. *Int. J. Photoenergy* **2013**, *2013*, 918025. [CrossRef]
139. Nasseh, N.; Arghavan, F.S.; Rodriguez-Couto, S.; Hossein Panahi, A.; Esmati, M.; A-Musawi, T.J. Preparation of Activated Carbon@ZnO Composite and Its Application as a Novel Catalyst in Catalytic Ozonation Process for Metronidazole Degradation. *Adv. Powder Technol.* **2020**, *31*, 875–885. [CrossRef]
140. Løgager, T.; Holcman, J.; Sehested, K.; Pedersen, T. Oxidation of Ferrous Ions by Ozone in Acidic Solutions. *Inorg. Chem.* **1992**, *31*, 3523–3529. [CrossRef]
141. Huaccallo-Aguilar, Y.; Álvarez-Torrellas, S.; Larriba, M.; Águeda, V.I.; Delgado, J.A.; Ovejero, G.; García, J. Optimization Parameters, Kinetics, and Mechanism of Naproxen Removal by Catalytic Wet Peroxide Oxidation with a Hybrid Iron-Based Magnetic Catalyst. *Catalysts* **2019**, *9*, 287. [CrossRef]
142. Barrault, J.; Abdellaoui, M.; Bouchoule, C.; Majesté, A.; Tatibouët, J.M.; Louloudi, A.; Papayannakos, N.; Gangas, N.H. Catalytic Wet Peroxide Oxidation over Mixed (Al–Fe) Pillared Clays. *Appl. Catal. B Environ.* **2000**, *27*, L225–L230. [CrossRef]
143. Mejbar, F.; Miyah, Y.; Benjelloun, M.; Ssouni, S.; Saka, K.; Lahrichi, A.; Zerrouq, F. High-Performance of Cu@eggshells for Toxic Dyes Catalytic Wet Peroxide Oxidation: Kinetics, Design of Experiments, Regeneration, and Cost Analysis. *Case Stud. Chem. Environ. Eng.* **2024**, *9*, 100572. [CrossRef]
144. Garcia-Mora, A.M.; Torres-Palma, R.A.; García, H.; Hidalgo-Troya, A.; Galeano, L.A. Removal of Dissolved Natural Organic Matter by the Al/Fe Pillared Clay-Activated-Catalytic Wet Peroxide Oxidation: Statistical Multi-Response Optimization. *J. Water Process Eng.* **2021**, *39*, 101755. [CrossRef]
145. Peralta, Y.M.; Sanabria, N.R.; Carriazo, J.G.; Moreno, S.; Molina, R. Catalytic Wet Hydrogen Peroxide Oxidation of Phenolic Compounds in Coffee Wastewater Using Al–Fe-Pillared Clay Extrudates. *Desalination Water Treat.* **2015**, *55*, 647–654. [CrossRef]
146. Balcı, S.; Tomul, F. Catalytic Wet Peroxide Oxidation of Phenol through Mesoporous Silica-Pillared Clays Supported Iron and/or Titanium Incorporated Catalysts. *J. Environ. Manag.* **2023**, *326*, 116835. [CrossRef]
147. Ben Achma, R.; Ghorbel, A.; Dafinov, A.; Medina, F. Copper-Supported Pillared Clay Catalysts for the Wet Hydrogen Peroxide Catalytic Oxidation of Model Pollutant Tyrosol. *Appl. Catal. A Gen.* **2008**, *349*, 20–28. [CrossRef]
148. Carriazo, J.; Guélou, E.; Barrault, J.; Tatibouët, J.M.; Molina, R.; Moreno, S. Catalytic Wet Peroxide Oxidation of Phenol by Pillared Clays Containing Al–Ce–Fe. *Water Res.* **2005**, *39*, 3891–3899. [CrossRef] [PubMed]
149. García-Mora, A.M.; Portilla-Delgado, C.S.; Torres-Palma, R.A.; Hidalgo-Troya, A.; Galeano, L.A. Catalytic Wet Peroxide Oxidation to Remove Natural Organic Matter from Real Surface Waters at Urban and Rural Drinking Water Treatment Plants. *J. Water Process Eng.* **2021**, *42*, 102136. [CrossRef]
150. Inchaurrondo, N.; Cechini, J.; Font, J.; Haure, P. Strategies for Enhanced CWPO of Phenol Solutions. *Appl. Catal. B Environ.* **2012**, *111–112*, 641–648. [CrossRef]
151. Li, C.; Zhu, N.; Yang, S.; He, X.; Zheng, S.; Sun, Z.; Dionysiou, D.D. A Review of Clay Based Photocatalysts: Role of Phyllosilicate Mineral in Interfacial Assembly, Microstructure Control and Performance Regulation. *Chemosphere* **2021**, *273*, 129723. [CrossRef] [PubMed]
152. Fox, M.A.; Dulay, M.T. Heterogeneous Photocatalysis. *Chem. Rev.* **1993**, *93*, 341–357. [CrossRef]
153. Hoffmann, M.R.; Martin, S.T.; Choi, W.; Bahnemann, D.W. Environmental Applications of Semiconductor Photocatalysis. *Chem. Rev.* **1995**, *95*, 69–96. [CrossRef]
154. Chakravorty, A.; Roy, S. A Review of Photocatalysis, Basic Principles, Processes, and Materials. *Sustain. Chem. Environ.* **2024**, *8*, 100155. [CrossRef]
155. Dlamini, M.C.; Maubane-Nkadimeng, M.S.; Moma, J.A. The Use of TiO_2/Clay Heterostructures in the Photocatalytic Remediation of Water Containing Organic Pollutants: A Review. *J. Environ. Chem. Eng.* **2021**, *9*, 106546. [CrossRef]
156. Sun, Z.; Lian, C.; Li, C.; Zheng, S. Investigations on Organo-Montmorillonites Modified by Binary Nonionic/Zwitterionic Surfactant Mixtures for Simultaneous Adsorption of Aflatoxin B1 and Zearalenone. *J. Colloid Interface Sci.* **2020**, *565*, 11–22. [CrossRef] [PubMed]
157. Aslam, U.; Rao, V.G.; Chavez, S.; Linic, S. Catalytic Conversion of Solar to Chemical Energy on Plasmonic Metal Nanostructures. *Nat. Catal.* **2018**, *1*, 656–665. [CrossRef]

158. Hariganesh, S.; Vadivel, S.; Maruthamani, D.; Rangabhashiyam, S. Disinfection By-Products in Drinking Water: Detection and Treatment Methods. In *Disinfection By-products in Drinking Water: Detection and Treatment*; Elsevier: Amsterdam, The Netherlands, 2020; pp. 279–304. [CrossRef]
159. Mishra, A.; Mehta, A.; Basu, S. Clay Supported TiO_2 Nanoparticles for Photocatalytic Degradation of Environmental Pollutants: A Review. *J. Environ. Chem. Eng.* **2018**, *6*, 6088–6107. [CrossRef]
160. Mori, K.; Kondo, Y.; Morimoto, S.; Yamashita, H. A Multifunctional Heterogeneous Catalyst: Titanium-Containing Mesoporous Silica Material Encapsulating Magnetic Iron Oxide Nanoparticles. *Chem. Lett.* **2007**, *36*, 1068–1069. [CrossRef]
161. Peñas-Garzón, M.; Gómez-Avilés, A.; Bedia, J.; Rodriguez, J.J.; Belver, C. Effect of Activating Agent on the Properties of TiO_2/Activated Carbon Heterostructures for Solar Photocatalytic Degradation of Acetaminophen. *Materials* **2019**, *12*, 378. [CrossRef] [PubMed]
162. Boudraa, R.; Talantikite-Touati, D.; Souici, A.; Djermoune, A.; Saidani, A.; Fendi, K.; Amrane, A.; Bollinger, J.C.; Nguyen Tran, H.; Hadadi, A.; et al. Optical and Photocatalytic Properties of TiO_2–Bi_2O_3–CuO Supported on Natural Zeolite for Removing Safranin-O Dye from Water and Wastewater. *J. Photochem. Photobiol. A Chem.* **2023**, *443*, 114845. [CrossRef]
163. Guo, J.; Fan, Y.; Dong, X.; Zeng, H.; Ma, X.; Fu, Y. Study on Preparation of UV-CDs/Zeolite-4A/TiO_2 Composite Photocatalyst Coupled with Ultraviolet-Irradiation and Their Application of Photocatalytic Degradation of Dyes. *J. Environ. Manag.* **2024**, *354*, 120342. [CrossRef] [PubMed]
164. Mehta, A.; Mishra, A.; Sharma, M.; Singh, S.; Basu, S. Effect of Silica/Titania Ratio on Enhanced Photooxidation of Industrial Hazardous Materials by Microwave Treated Mesoporous SBA-15/TiO_2 Nanocomposites. *J. Nanopart. Res.* **2016**, *18*, 209. [CrossRef]
165. Ji, H.; Liu, W.; Sun, F.; Huang, T.; Chen, L.; Liu, Y.; Qi, J.; Xie, C.; Zhao, D. Experimental Evidences and Theoretical Calculations on Phenanthrene Degradation in a Solar-Light-Driven Photocatalysis System Using Silica Aerogel Supported TiO_2 Nanoparticles: Insights into Reactive Sites and Energy Evolution. *Chem. Eng. J.* **2021**, *419*, 129605. [CrossRef]
166. Zhao, S.; Qi, Y.; Lv, H.; Jiang, X.; Wang, W.; Cui, B.; Liu, W.; Shen, Y. Effect of Clay Mineral Support on Photocatalytic Performance of BiOBr-TiO_2 for Efficient Photodegradation of Xanthate. *Adv. Powder Technol.* **2024**, *35*, 104431. [CrossRef]
167. Pérez-Carvajal, J.; Aranda, P.; Obregón, S.; Colón, G.; Ruiz-Hitzky, E. TiO_2-Clay Based Nanoarchitectures for Enhanced Photocatalytic Hydrogen Production. *Microporous Mesoporous Mater.* **2016**, *222*, 120–127. [CrossRef]
168. Mishra, A.; Mehta, A.; Sharma, M.; Basu, S. Enhanced Heterogeneous Photodegradation of VOC and Dye Using Microwave Synthesized TiO_2/Clay Nanocomposites: A Comparison Study of Different Type of Clays. *J Alloys Compd.* **2017**, *694*, 574–580. [CrossRef]
169. Sangare, S.; Belaidi, S.; Saoudi, M.; Bouaziz, C.; Seraghni, N.; Sehili, T. Iron-TiO_2 Pillared Clay Nanocomposites: Eco-Friendly Solutions for Photocatalytic Removal of Organic and Pathogen Contaminants. *Inorg. Chem. Commun.* **2024**, *160*, 111923. [CrossRef]
170. Yusuff, A.S.; Olateju, I.I.; Adesina, O.A. TiO_2/Anthill Clay as a Heterogeneous Catalyst for Solar Photocatalytic Degradation of Textile Wastewater: Catalyst Characterization and Optimization Studies. *Materialia* **2019**, *8*, 100484. [CrossRef]
171. Hass Caetano Lacerda, E.; Monteiro, F.C.; Kloss, J.R.; Fujiwara, S.T. Bentonite Clay Modified with Nb2O5: An Efficient and Reused Photocatalyst for the Degradation of Reactive Textile Dye. *J. Photochem. Photobiol. A Chem.* **2020**, *388*, 112084. [CrossRef]
172. Tobajas, M.; Belver, C.; Rodriguez, J.J. Degradation of Emerging Pollutants in Water under Solar Irradiation Using Novel TiO_2-ZnO/Clay Nanoarchitectures. *Chem. Eng. J.* **2017**, *309*, 596–606. [CrossRef]
173. Carriazo, J.G.; Moreno-Forero, M.; Molina, R.A.; Moreno, S. Incorporation of Titanium and Titanium–Iron Species inside a Smectite-Type Mineral for Photocatalysis. *Appl. Clay Sci.* **2010**, *50*, 401–408. [CrossRef]
174. Paul, B.; Martens, W.N.; Frost, R.L. Immobilised Anatase on Clay Mineral Particles as a Photocatalyst for Herbicides Degradation. *Appl. Clay Sci.* **2012**, *57*, 49–54. [CrossRef]
175. Damardji, B.; Khalaf, H.; Duclaux, L.; David, B. Preparation of TiO_2-Pillared Montmorillonite as Photocatalyst Part II: Photocatalytic Degradation of a Textile Azo Dye. *Appl. Clay Sci.* **2009**, *45*, 98–104. [CrossRef]
176. Li, C.; Sun, Z.; Huang, W.; Zheng, S. Facile Synthesis of G-C_3N_4/Montmorillonite Composite with Enhanced Visible Light Photodegradation of Rhodamine B and Tetracycline. *J. Taiwan Inst. Chem. Eng.* **2016**, *66*, 363–371. [CrossRef]
177. Fatimah, I.; Syu'aib, Y.; Ramanda, G.D.; Kooli, F.; Sagadevan, S.; Oh, W.C. Facile Synthesis of Highly Active and Reusable NiO/Montmorillonite Photocatalyst for Tetracycline Removal by Photocatalytic Oxidation. *Inorg. Chem. Commun.* **2025**, *172*, 113731. [CrossRef]
178. Abdennouri, M.; Baâlala, M.; Galadi, A.; El Makhfouk, M.; Bensitel, M.; Nohair, K.; Sadiq, M.; Boussaoud, A.; Barka, N. Photocatalytic Degradation of Pesticides by Titanium Dioxide and Titanium Pillared Purified Clays. *Arab. J. Chem.* **2016**, *9*, S313–S318. [CrossRef]
179. Pourmadadi, M.; Aghababaei, N.; Abdouss, M. Performance and Reaction Mechanism of Montmorillonite/α-Fe_2O_3/Starch Bio-Nanocomposite as High-Efficiency Photocatalytic Degradation of Acetaminophen: Characterization, Feasibility, and Pathway. *Int. J. Biol. Macromol.* **2024**, *279*, 135363. [CrossRef] [PubMed]
180. González, B.; Trujillano, R.; Vicente, M.A.; Rives, V.; Korili, S.A.; Gil, A. Photocatalytic Degradation of Trimethoprim on Doped Ti-Pillared Montmorillonite. *Appl. Clay Sci.* **2019**, *167*, 43–49. [CrossRef]

181. Cardona, Y.; Węgrzyn, A.; Miśkowiec, P.; Korili, S.A.; Gil, A. Catalytic Photodegradation of Organic Compounds Using TiO_2/Pillared Clays Synthesized Using a Nonconventional Aluminum Source. *Chem. Eng. J.* **2022**, *446*, 136908. [CrossRef]
182. Liang, Y.; Li, W.; Bei, B.; Li, C.; He, Z.; Wang, X.; Zhou, R.; Ding, H.; Li, S. Composites of TiO_2 Pillared Sericite: Synthesis, Characterization and Photocatalytic Degradation of Methyl Orange. *Appl. Clay Sci.* **2023**, *242*, 107044. [CrossRef]